Charles University in Prague

Faculty of Science

Developmental and Cell Biology

MSci. Michal Dvořan

Characterization of translational patterns in mammalian oocytes and early embryos obtained under different conditions

Charakterizace translačních profilů v savčích oocytech a časných embryích získávaných za různých podmínek

Doctoral Thesis

Supervisor: Ing. Michal Kubelka CSc.

Co-supervisor: Ing. Andrej Šušor Ph.D.

Institute of Animal Physiology and Genetics, Czech Academy of Sciences

Libechov, 2023

Prohlášení

Prohlašuji, že jsem závěrečnou práci zpracoval samstatně a že jsem uvedl všechny použité informační zdroje a literaturu. Tato práce, ani její podstatná část, nebyla předložena k získání jiného nebo stejného akademického titulu.

I hereby declare that I wrote this thesis independently, using the cited literature. This work or a substantial part of it has not been submitted elsewhere to obtain any other academic degree.

V Liběchově dne 30.10.2023 *Michal Dvořan*

Acknowledgement

I would like to express my warmest thanks to the current and former members of the Laboratory of Biochemistry and Molecular Biology of Germ Cells at Institute of Animal Physiology and Genetics in Libechov, particularly to the head of the laboratory, Ing. Andrej Susor Ph.D. for his immense professional as well as personal support throughout the years as well as to my supervisor Ing. Michal Kubelka CSc., former colleagues, post-doc MSc. Rajan Iyyappan Ph.D., former Ph.D. student MSc. Edgar del Llano Ph.D and MSc. Daria Aleshkina Ph.D. and current post-doc Mgr. Denisa Jansova Ph.D.

Let me also express my deepest gratitude to the loving, caring and indispensable lab technicians Jaroslava Supolikova and Marketa Hancova.

Table of Contents

Abstract

Fully grown mammalian oocytes collected from stimulated follicles spontaneously resume meiotic maturation *in vitro* and progress towards the metaphase II stage of meiosis. Matured ''egg'' becomes fertilized, accommodates paternal genome, and develops into an early embryo. All these processes are accompanied by temporarily ceased transcription. Following meiotic resumption, oocytes and early embryos rely exclusively on stored maternal transcripts and their effective utilization by spatiotemporally regulated translation. My doctoral thesis uncovers differences in translation patterns under different conditions, *in vitro* and *in vivo* maturation of mouse oocytes and respectively derived early embryos. The thesis is tailored to assisted reproduction technology relevant *in vitro* maturation conditions as well as respectively produced *in vitro* fertilized oocytes. An investigation into molecular processes behind deregulated actively translated transcripts is much needed to identify factors responsible for compromised developmental competency of *in vitro* matured oocytes. Low success rates often deter patients from choosing *in vitro* maturation, however, it may confer an advantage for patients suffering from Polycystic Ovarian Syndrome or may serve as a bypass for those at high risk of developing severe Ovarian Hyper Stimulation Syndrome. These findings could instigate further clinical research into improving *in vitro* maturation technology, not only for the benefit of small groups of patients, but also for future applications in fertility preservation.

Abstrakt (česky)

Savčí oocyty získané ze stimulovaných folikulů spontánně obnovují meiotickou maturaci *in vitro*, po které se zastaví až v metafázi II. meiotického dělení. Zralé vajíčko je následně fertilizováno, dojde k inkorporaci paternálního genomu a vývoji v časné embryo. Všechny tyto procesy jsou doprovázeny dočasným umlčením transkripce. Po znovuzahájení meiózy jsou oocyty a časná embrya odkázány na efektivní využití uložených maternálních transkriptů prostřednictvím translace, která je regulována v prostoru a čase. Moje dizertační práce charakterizuje rozdíly v translačních profilech za různých podmínek *in vitro* a *in vivo* maturace myších oocytů a analogicky získaných časných embryí. Tato práce je zaměřena jak na studium klinicky relevantních kultivačních podmínek *in vitro* maturace používaných v asistované reprodukci, tak i na studium takto získaných *in vitro* fertilizovaných oocytů. Výzkum těchto procesů na molekulární úrovni, které stojí za deregulací aktivně translatovaných transkriptů je důležitý pro identifikaci faktorů, které jsou zodpovědné za sníženou vývojovou kompetenci *in vitro* maturovaných oocytů. Nízká úspěšnost *in vitro* maturace často odrazuje pacienty, ale zároveň může představovat výhodu pro pacienty trpící syndromem polycystických ovárií nebo alternativu pro ženy s vysokým rizikem ovariálního hyperstimulačního syndromu. Výsledky této práce mohou podnítit související klinický výzkum vylepšující metodu *in vitro* maturace nejen pro úzkou skupinu pacientek, ale také pro budoucí metody zachování plodnosti.

1. Introduction

1.1 Oocyte and early embryo development *in vivo*

Sexual reproduction via germ cells ensure continuity of generations in many species. In rapidly changing living environments and lifestyle, various factors influence their fertility. As a response to this threat, *in vitro* techniques for fertility preservations have been developed. However, in order to preserve the highest developmental potential of the germ cells, it is crucial to understand the molecular processes underlying the *in vivo* development. As this thesis is focused on oocytes and early embryos, their *in vivo* development is categorized into a follicle development accompanied by oocyte growth, meiotic resumption and maturation into an MII oocyte (an Egg), fertilization and early embryo development, ranging from zygote up to the blastocyst stage. Further *in vivo* processes including blastocyst hatching, nidation into an endometrial wall or embryonic development are out of the scope of this thesis.

Female germ cells, the oocytes, are developing within follicles originated from an ovarian cortex. Primordial follicle recruitment for maturation is governed hormonally. A woman before its birth has about 1-2 million oocytes, however the numbers are continuously decreasing towards puberty leaving around 300 000 oocytes for the reproductive life (Bromfield and Piersanti, 2019). Upon signals retrieved from hypothalamus-anterior pituitary axis (Fig. 1), a small cohort of primordial follicles harbouring oocytes are recruited for maturation.

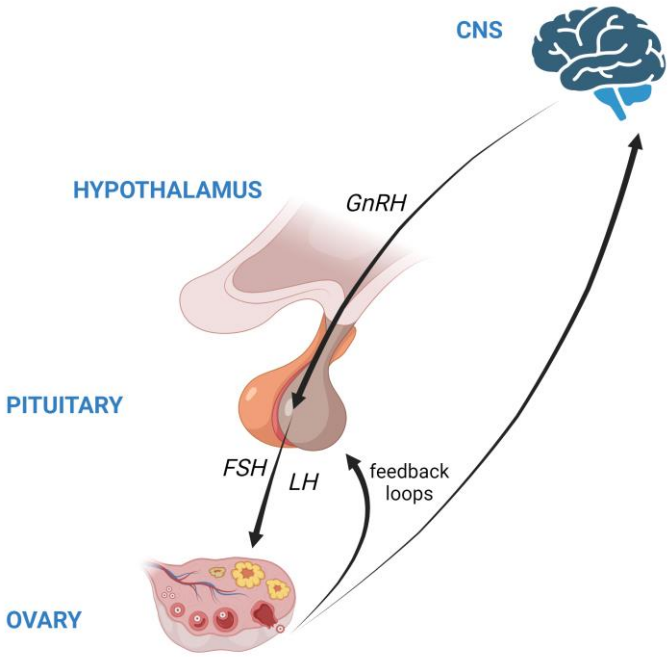

Fig. 1 Hypothalamus-Pituitary-Ovarian Axis. Upon signals retrieved from the central nervous system (CNS), the gonadotropin-releasing hormone (GnRH) is synthesized in hypothalamus. Pulse frequencies of GnRH are responsible for stimulating secretion of follicle-stimulating hormone (FSH) and luteinizing hormone (LH) as well as the feedback loops by androgens and estrogens (Bromfield and Piersanti, 2019) (Created with BioRender.com) .

Oocytes are created during intrauterine embryonic development by the process of oocytogenesis, which is driven by mitosis. Before the birth, primordial follicles are formed within ovarian cortex containing primary oocytes, which are arrested in the Diplotene stage of prophase I meiotic division. This meiotic arrest is maintained until puberty, when the hypothalamus-pituitary-ovarian axis (Fig.1) is fully matured. Within 2-3 years from the first menstrual cycle adult hormonal values of FSH and LH are achieved and primary oocytes are gradually recruited for maturation (Carlson and Shaw, 2019). Oocyte growth within primary and secondary follicles is controlled by various factors, for example, indirectly by oocyte-secreted factors: growth differentiation factor 9, bone-morphogenic protein 15 from transforming growth factor β superfamily that instigate somatic cell growth within follicles in a paracrine fashion (Paulini and Melo, 2011) or directly by, for example, kit ligand or leukaemia inhibitory factor (Paulini and Melo, 2011). Follicle growth is also dependent on insulin, progesterone or anti-Mullerian hormone. The last one is commonly utilized for the clinical assessment of ovarian reserve as it is produced by granulosa cells within growing follicles (Moolhuijsen and Visser, 2020).

Since the oocyte has started growing, the process of rapid transcript accumulation is running, aided by surrounded somatic cells. Growing or so called non-surrounded nucleolus (NSN) germinal vesicle (GV) oocyte is still involved in this process with active transcription until the chromatin changes morphology (Sun *et al.*, 2023) to so called surrounded nucleolus (SN). At this point, the GV oocyte is fully grown and its transcription is ceased (Susor and Kubelka, 2017). Upon the sudden increase in pulse frequency of gonadotropin-relasing hormone (GnRH), a surge of luteinizing hormone (LH) is released from the anterior pituitary gland. As a consequence, sequences of events are triggered to resume oocyte meiotic division following the arrest in the Diplotene of prophase I (Bromfield and Piersanti, 2019). Stimulation of luteinizing hormone receptor on mural granulosa cells by LH surge is followed by its endocytosis, to prevent continuous stimulation (Pan and Li, 2019) , and upregulating expression of epidermal-growth factor-like (EGF-like) peptides, amphiregulin, epiregulin and betacellulin. They increase the expression of extracellular-signal regulated kinase 1 (ERK1) also known as mitogen-activated-protein kinase 3 and also bind to their EGF receptor. The key effect of these changes is the cessation of cyclic guanosine-monophoshate (cGMP) production, its effusion from within the oocyte and orchestrated closure of connexins located in gap junctions (Shuhaibar *et al.*, 2015). cGMP is responsible for the inhibition of phosphodiesterase 3A, an enzyme that degrades cyclic adenosine-monophoshate (cAMP). Gradual concentration decline of cGMP in oocyte's cytoplasm is accompanied by faster cAMP degradation that results in protein kinase A (PKA) inhibition. Inhibition of PKA then allows promotion of the nuclear envelope breakdown (NEBD) via activated maturation-promoting factor (MPF). MPF is a protein dimer composed of cyclin B1 (CCNB1) and cyclin dependent kinase 1 (CDK1) (Fan and Sun, 2019).

Ongoing meiotic maturation, activated by MPF, is exclusively dependent on correct resource management by various mechanisms regulating translation of stored maternal transcripts. Functional transcription is temporarily ceased not only along meiotic maturation, but also at fertilization and during minor zygotic genome activation. The restoration of the functional transcriptional activity does not happen until the 2-cell stage in the mouse model and 8-cell stage in humans, when embryonic genome is activated (Yan *et al.*, 2013). It is worth mentioning that recent results have demonstrated that a certain basal level of embryonic transcriptional activity was observed as early as zygote stage in humans (Asami *et al.*, 2022). Meiotic maturation includes completion of Meiosis I, 1st polar body extrusion (PBE) and formation of matured MII oocyte, also called „an Egg". To create a developmentally competent egg, two parts of meiotic maturation have to be accomplished, both nuclear and cytoplasmic (Fan and Sun, 2019). Completion of nuclear maturation is postponed with regard to the 1st PBE and it has already been suggested to reflect this phenomenon in assisted reproduction (AR) to increase fertilization rates (FR) (Holubcová *et al.*, 2019). On the other hand, cytoplasmic maturation is much less defined as it entails everything else within the oocyte, e.g. the state of transcriptome and proteome. Cytoplasmic maturation is also energy dependent and can be negatively affected by reactive oxygen species (ROS) (Xie *et al.*, 2018). A couple of years ago, an ultrastructural study suggested to employ a morphological map for evaluating cytoplasmic maturity in human MII oocytes (Trebichalská *et al.*, 2021). Cytoplasmic maturation can also be supported by surrounding cumulus cells. However, in the final moments before ovulation of *in vivo* oocytes (IVO), cumulus-oocyte complex (COC) communication via transzonal projections (TZPs) is ceased and somatic TZPs are retracted by ERK-mediated loss of filopodial adhesion and its shortening. (Abbassi *et al.*, 2021). However, cumulus cells still remain attached to the oocyte until fertilization, synthesizing hyaluronan complexes within cumulus extracellular matrix by trans-esterification reactions in presence of serum-derived inter-alpha-trypsin inhibitor (Nagyová, Němcová and Camaioni, 2022). Increasing pressure of expanding COC, thinning and vascularization of follicular wall (Fig.10) results in ovulation and transfer of ovulated COCs into oviducts (Russell and Robker, 2019).

Ovulated, developmentally competent, IVO COCs interact with oviductal cells. This interaction is increasing the expression of C-natriuretic peptide, which signals to release capacitated sperm from the isthmic reservoir and let COCs to become fertilized (Wang *et al.*, 2022). Sperm that are destined to fertilize oocytes have to undergo initial maturation within epididymis of male's reproductive system and are stored prior to ejaculation in cauda. Upon sexual intercourse, sperm is released via ductus deferens into female's reproductive tract, where is further capacitated. It is now getting attention that along hereinabove described journey of sperm towards oocytes, extracellular vesicles (EVs) are present and take part in capacitating sperm, as demonstrated in a bovine model (Franchi *et al.*, 2020). Fertilized embryos are also subjected to EVs interaction with oviductal wall along the travel into the uterus (Li *et al.*, 2023). These interactions are almost impossible to mimic in *in vitro* systems, however many novel approaches attempting to simulate this phenomenon are under investigation.

1.2 Oocyte and early embryo development *in vitro*

In vitro systems have been researched and developed with aim to study and treat infertility or in recent years to preserve fertility. Many *in vitro* models were devised analogically to almost every stage of *in vivo* development, starting from *in vitro* follicle culture, through *in vitro* maturation, fertilization, embryo development till the 14-day post-implantation embryo (Oldak *et al.*, 2023). *In vitro* follicle culture was studied extensively in a mouse model (O'Brien, Pendola and Eppig, 2003) as well as mechanisms related to folliculogenesis involving protein kinase B (PKB/AKT) and mechanistic target of rapamycin (mTOR) signalling pathways (Rehnitz *et al.*, 2017). However, the most prominent and clinically applied *in vitro* technologies in ART are *in vitro* fertilization or intracytoplasmic sperm injection (ISCI) coupled with *in vitro* early embryo development until the blastocyst stage (Fig. 2). Less common and often abandoned ART is *in vitro* meiotic maturation (IVM), which will be discussed in more detail below. The latest ART, which is becoming more common, is the ovarian tissue cryopreservation that is focused on fertility preservation (Fig.2). However, this technology is reliant on either exclusive *in vitro* maturation of thawed grafted tissue or its heterotopic or orthotopic transplantation. Downside of the former approach is that this IVM protocol is still under investigation, and the latter, graft transplantation approach, is prone to ischemia due to the lack of neovascularization (Dolmans *et al.*, 2021). Commonly adopted preservation in ART is cryopreservation by vitrification, which is a term for an imminent shock-freeze in liquid nitrogen. It is routinely performed in *in vitro* cultured human blastocysts, and less often in MII oocytes, which are in the majority of cases *in vitro* matured from collected GV oocytes.

IVM processes were mostly studied using mouse, bovine or porcine models. Sometimes, human oocytes were used, however, they were usually of low quality and in most cases retrieved from already ovulated follicles. Routinely fully grown GV oocytes enter IVM as COCs or as denuded oocytes (DO). To synchronize GV oocyte population ahead of NEBD and eliminate NSN GV oocytes prior to meiotic maturation, high cAMP levels within oocyte's cytoplasm are maintained by either inhibiting phosphodiesterase 3A or stimulating adenylate cyclase. Upon release for maturation, supported cAMP elevation is rapidly ended (Bromfield and Piersanti, 2019). Further success of IVM is heavily dependend on culture conditions, which differ with regard to the presence of absence of somatic cells.

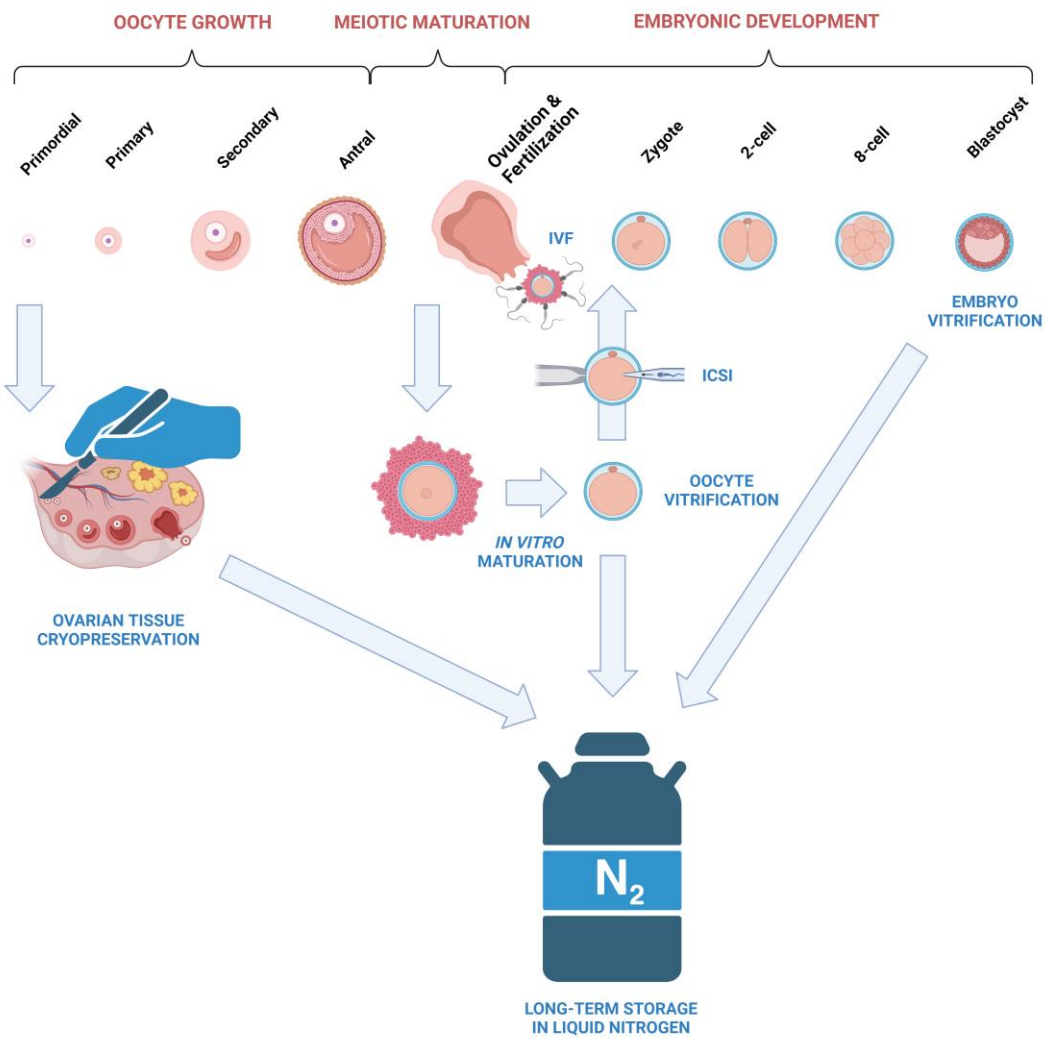

Fig. 2 Means of fertility preservation along oocyte maturation and early embryo development. Three key stages of fertility preservation do exist along the process of oocyte maturation. At the initial stage, ovarian tissue containing primordial follicles has recently been devised to preserve fertility of young women. Later in the maturation, fully grown germinal vesicle oocytes could undergo maturation *in vivo* upon rhCG trigger or *in vitro* and become cryopreserved once reach fully matured MII oocyte stage. The third stage is blastocysts vitrification obtained from conventional *in vitro* fertilization and *in vitro* embryo culture (Created with BioRender.com).

Clinical IVM media are conventionally supplemented with amino acids, vitamins and human serum albumin. Also, recombinant gonadotropins, rFSH and rLH or rhCG are administered shortly before the actual maturation and at equal concentrations corresponding to roughly 5 ng/mL (Wang, Ock and Chian, 2006). Previous findings demonstrated that administration of rFSH itself to IVM medium at about 20 times higher concentration is significantly affecting global translation in oocytes across all mammalian model species, including human (Tetkova *et al.*, 2019). Supplementation of IVM media with human serum is not legally acceptable in the clinical environment, even though it may pose a significant improvement to the IVM. Therefore the only option is the use of human serum albumin or a synthetic serum substitute (Yang *et al.*, 2021). Also, the assessment of egg maturity *in vitro* is problematic. The only known method to assess the completion of nuclear maturity in ART is the use of Polarized Light Microscopy (Nguyen Thanh, Doan Thi and Quan Hoang, 2018). Means of assessing cytoplasmic maturity are still in the process and are not yet properly

defined. In mice it is known that MII spindles of IVM oocytes are barrel-shaped compared to IVO (Sanfins *et al.*, 2003), which is accompanied by not focused spindle poles. The correct microtubule-kinetochore attachment is also affected by IVM and often chromosomes are not properly aligned to the metaphase plate of MII spindle (Sanfins *et al.*, 2004). Completion of meiotic maturation and achieving the developmental competence is also energetically demanding or prone to oxidative or heat stress and therefore adequate maturation conditions have to be set in order to improve FR (Xie *et al.*, 2018).

The standard clinical fertilization protocol is to subject eggs to ICSI or IVF. IVF is the oldest ART, but still quite often unsuccessful for unknown reasons. Because of this, there is a preference for ICSI with performing IVF as the second option. Needless to say, IVF media and further embryo cultivation media are well designed with proven effectiveness. What is lacking, is the understanding of changes in cytoplasmic maturity upon IVF. Cytoplasmic maturity is tightly connected with changes in spatiotemporal organelle localization, stored maternal RNA metabolism and eventually changes in translatome (Jones *et al.*, 2008; Trebichalská *et al.*, 2021). Investigations into the improvement of consecutive *in vitro* embryo culture today is aimed at changes occurring under cultivation in normoxic or hypoxic conditions (Houghton, 2021), single or grouped embryo culture (Fancsovits *et al.*, 2022) or the effect of EVs derived from oviductal fluid of *in vitro* cultivated tissue (Li *et al.*, 2023). Experimental *in vitro* embryo-like systems, the „embryoids“ were recently developed (Harrison, Sozen and Zernicka-Goetz, 2018), which could in the future replace some experiments performed today on animal models. A breakthrough in *in vitro* maturation technology were mouse oocytes and embryos originated from embryonic and adult tail tip fibroblasts. Once transferred, got implanted and became viable mice pups (Hikabe *et al.*, 2016).

1.3 Mediocre oocyte *in vitro* maturation technology in assisted reproduction

Clinically speaking, the conventional process of *in vitro* meiotic maturation (IVM) is one of the treatment options, however, due to unsatisfactory fertilization and live-birth rates, it is reluctantly adopted (Yang *et al.*, 2021).

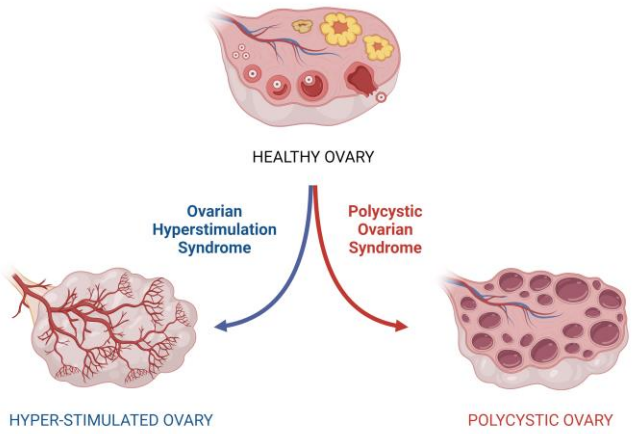

Fig. 3 Clinical pathogies manageable or aviodable by *in vitro* maturation technology. Two major patient groups seeking infertility treatment could benefit from *in vitro* maturation technology. Patients suffering from Polycystic Ovarian syndrome produce a large amount of immature oocytes, which could become eggs only by applying *in vitro* maturation. The second group of patients benefiting from in vitro maturation are those who are at high risk of severe Ovarian Hyperstimulation Syndrome, which, if not treated, increases vascular perfusion and may lead to life-threatening intraperitoneal bleeding (Created with BioRender.com).

As recently stated upon complex meta-analysis, it is less effective than standard IVF/ICSI, but may be advantageous for patients suffering from Polycystic Ovarian Syndrome (PCOS), an endocrine disorder, or for those, who suffer from Ovarian Hyperstimulation Syndrome (OHSS) (Fig. 3) (Teede *et al.*, 2023). About 20% of female patients attending fertility clinics are diagnosed with PCOS. PCOS patients produce excessive amount of immature GV oocytes. The background of this syndrome is multifactorial with both genetic and environmental triggers (Dvoran, Nemcova and Kalous, 2022). Conventional IVM is an optional treatment for these patients, however, with questionable outcomes (Rodrigues *et al.*, 2023). The secondly mentioned syndrome, the OHSS, is even more common in patients undergoing standard IVF cycles. OHSS has life threatening repercussions if overlooked and not treated within time. It is manifested by increased vascular perfusion throughout ovaries that can lead towards intraperitoneal bleeding. In both cases, IVM may be advantageous for these patients (ESHRE, 2016).

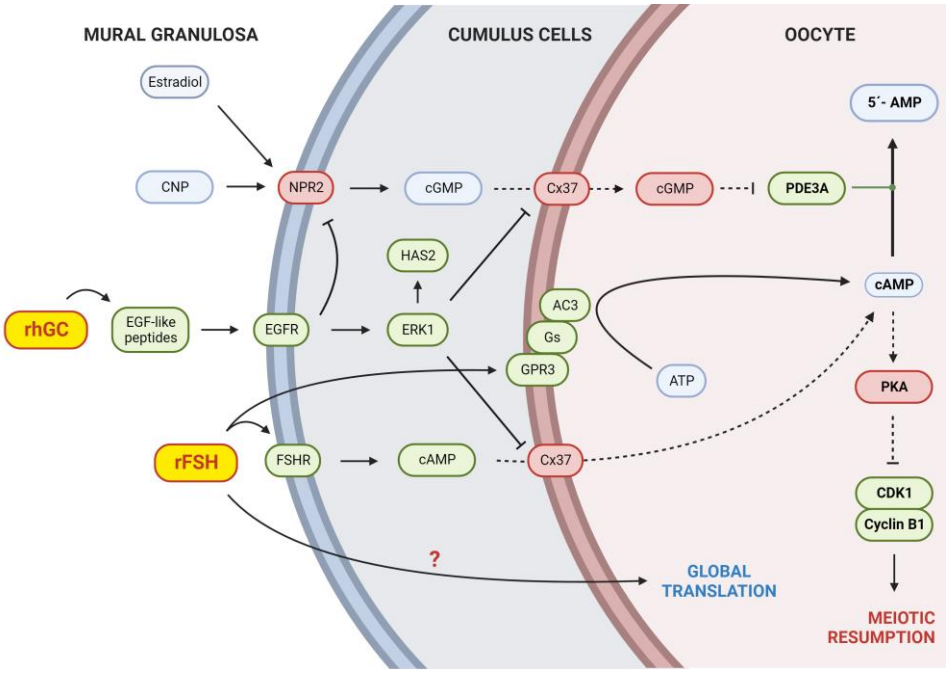

Fig. 4 Recombinant gonadotropins mode of action on *in vitro* cultured cumulus-oocyte complex. The action of recombinant follicle-stimulating hormone (rFSH) and recombinant human chorionic gonadotropin (rhCG), an analog of luteinizing hormone (LH), on the meiotic resumption in an *in vitro* cultured cumulus-oocyte complex. (Richani and Gilchrist, 2018)(Created with BioRender.com)

Recombinant gonadotropins, rFSH and rhCG (Fig. 4) are standardly added to αMEM medium with amino acids, vitamins and bovine serum albumin to support cumulus-oocyte complex growth *in vitro*. This system, however imperfect, has about 50% oocyte maturation rate with little better outcomes following the rhGC priming before the actual GV collection. IVM live birth rate (LBR) is about 30% (Chian *et al.*, 2023). rFSH is able to transiently increase cAMP concentrations within COCs by increasing the activity of G-protein coupled receptor 3 and adjacent adenylate cyclase. If gap junctions were closed, the rFSH effect ceased (Li, Mao and Xia, 2012). The second gonadotropin rhCG, an analogue of LH, is responsible for efflux of cyclic guanosine monophosphate (cGMP) out of oocyte and gap junctions closure among cumulus cells (Shuhaibar *et al.*, 2015). Taken together, administration of both rFSH and rhCG on COCs could have only mild effect on

granting additional time to prevent premature NEBD. The question is to what extent this IVM culture setting can improve collected COC developmental potential, particularly with respect to IVM of DO.

1.4 Translation in mammalian oocytes and early embryos

The importance of translation and its correct spatiotemporal regulation for oocyte maturation and early embryo development, has already been stressed and key points were outlined. The progression of developmental processes is exclusively translation-based, since transcription is silenced during the period from fully grown, SN GV oocyte up to the embryonic genome activation (Fig. 5). Translational regulation is managed by various processes within oocyte and embryo cytoplasm. The mTOR complex 1 (mTORC1), a kinase that is involved in oocyte growth upon nutrient availability, is employed in translational regulation of transcripts with 5‘-terminal oligopyrimidine (TOP) motifs. These mRNA transcripts are regulated by cap-dependent translation via interactions between cap-binding proteins eIF4E, eIF4G1 and their regulator 4E-BP1, which activity is regulated by mTORC1 phosphorylation (Thoreen *et al.*, 2012). In oocytes it was observed that during meiotic maturation mTOR-eIF4F machinery is active and spatially localized around chromosomes and spindle (Susor *et al.*, 2015). Apart from cap-dependent translational activation, mRNA transcript quiescence is also regulated by differential polyadenylation of 3‘-untranslated regions (3‘-UTR). Every 3‘-UTR contain a polyadenylation signal that is bound by the cleavage and polyadenylation specificity factor. Further towards the 3‘-end, a variable number of cytoplasmic polyadenylation elements are present. The closer the distance between those two regions within the 3‘-UTR, the stronger translational repression is (Dai *et al.*, 2019). Cytoplasmic polyadenylation elements are bound by cytoplasmic polyadenylation binding proteins, which control translation induced by polyadenylation (Jansova *et al.*, 2018). The kinetics of stored maternal transcriptome within oocytes and the availability of particular transcripts for translation is also simply regulated by selective decay mechanisms. As oocytes progress through meiosis, no longer required transcripts are selectively degraded, for example ribosomal RNA or GV-related transcripts (Su *et al.*, 2007). Apart from the specificity, the rate of RNA degradation and its proper timing with regard to the frequency of codon usage by translation machinery is also important (Despic and Neugebauer, 2018). An additional level to mRNA clearance is the epitranscriptomic regulation, where series of writers, readers and erasers function to orchestrate the dynamics of RNA modifications (Dvoran, Nemcova and Kalous, 2022). As a recent example, it was shown that downregulation of Mettl3, N6-methyladenosine methyltransferase, in the GV oocyte is inhibiting mRNA decay and the 1st PBE (Y. Zhu *et al.*, 2022). Another form of translational regulation is the hiding of transcripts from the translation machinery by storing them in a variety of ribonucleoprotein (RNP) particles such as P-bodies (PB) or stress granules (SG). P-bodies are non-membranous cytosolic organelles, which are formed from RNA and proteins by liquid-liquid transition. PBs can harbour on a large scale mRNAs of various functions, for instance transcripts involved in regulatory functions (Standart and Weil, 2018). Highly dynamic RNPs in form of stress granules are of similar nature to

PBs, but contain transcripts with stalled translation initiation, which are frequently shuttled in and out. SGs are liquid-like droplets with clear differentiation from other RNP forms, employed in stress response, apoptosis or cell signalling (Marcelo *et al.*, 2021).

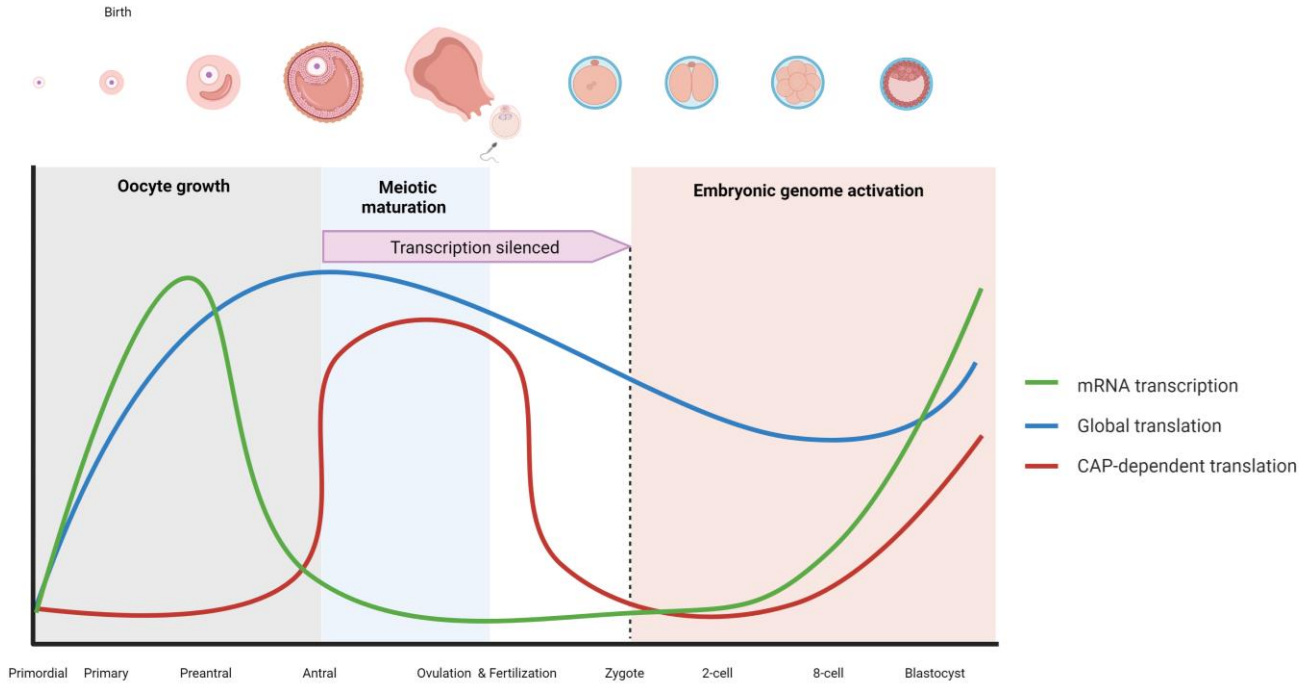

Fig. 5 mRNA transcription, global and cap-dependent translation kinetics along oocyte maturation, fertilization and early embryo development. Oocytes accumulate mRNA transcripts within their cytoplasm as they grow enclosed by adjacent granulosa cells of somatic origin. Once germinal vesicle oocytes reach fully grown surrounded nucleolus configuration, transcription is temporarily ceased. CAP-dependent translation is up-regulated from the point of meiotic resumption until the 2-cell stage (in mice). Global translation is, however, slowly decreasing from oocyte towards 8-cell stage embryo (Susor and Kubelka, 2017) (Created with BioRender.com).

Recently, it was reported that even another form of RNPs exist. It is mammalian specific, present in oocytes, and located in the vicinity of mitochondria. Therefore, it was named mitochondria-associated ribonucleoprotein domain (MARDO). The core nucleating component, RNA binding protein ZAR1, is dissolved upon transition from meiosis I to meiosis II to ensure timely degradation of translationally repressed transcripts previously clustered within MARDO (Cheng *et al.*, 2022).

All hereinabove mentioned translational regulations are reflected in changes to global translation, which is slowly, but gradually decreasing from the meiotic resumption until the embryonic genome activation (Susor and Kubelka, 2017) (Fig.5)

1.5 Monitoring selective recruitment of stored maternal transcripts by translational machinery

As it was already mentioned, the stored maternal transcriptome behaviour along the oocyte meiotic maturation, fertilization and early embryo development is highly dynamic, restructuralized and spatiotemporally trafficked (Marcelo *et al.*, 2021). Finely regulated translatome, the key to the completion of cytoplasmic maturation and achievement of the developmental competence, is vitally dependent on the availability of specific mRNA transcripts that must be accessible for translation machinery to be „actively“

translated in time and space. To explore this particular phenomenon, actively translated transcripts have to be refined from the stored maternal transcriptome.

The solid approach is to perform polysome fractionation by ultracentrifugation on a sucrose gradient (Fig. 6). However, the standard assay is demanding with respect to the amount of input material, to be able to analyse fractionated samples by absorbance reading.

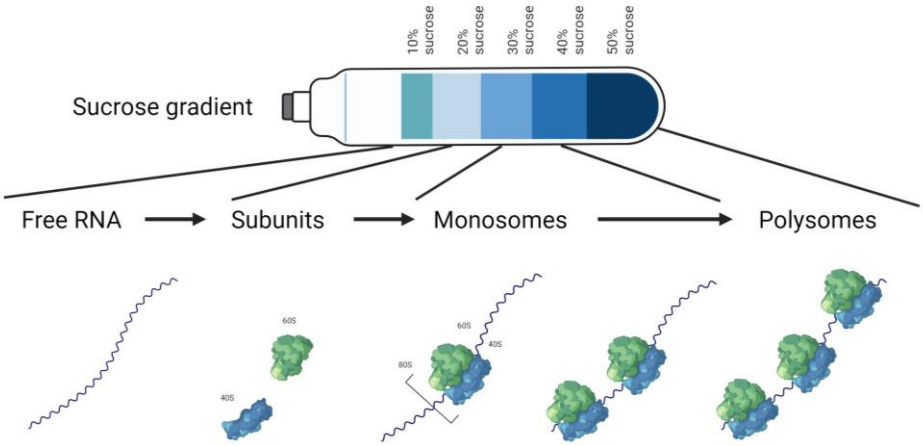

Fig. 6 Polysome fractionation by ultracentrifugation on a sucrose gradient is a common approach to extract transcripts actively involved in translation. Collected samples in the presence of cycloheximide, an inhibitor of translation elongation, were processed by ultracentrifugation on a 10 – 50 % sucrose gradient. Fractions containing polysome-bound transcripts were containing the highest gradient sucrose concentrations. In contrast, the lighest fractions contained free RNA molecules. The intermediate gradient part was abundant in free ribosomal subunits and monosomes (Created with BioRender.com).

To be able to fractionate samples at very low input amounts, like oocytes or embryos definitely are, an altered protocol named the Scarce Sample Profiling (SSP) was developed some years ago (Masek *et al.*, 2020), yielding decent amount of fractionated total RNA and credible results by further RNA-seq analysis (L. Zhu *et al.*, 2022). It is fair to mention, that newer alternatives to standard polysome profiling have been devised, like the RiboTag system (Sanz *et al.*, 2019) or Ribosomal Footprinting (Ingolia, 2016) , however both these assays have their limitations.

By means of the SSP assay and further RNA-seq analysis, polysome bound „actively“ translated transcripts present in MII oocytes and pronuclear zygotes under various clinically relevant culture conditions can be monitored.

2. Aims of the Thesis

In general, the overall goal of this thesis is to **map differences in recruitment of stored maternal transcripts by oocyte or embryo translation machinery**. Experimental data acquisition was done via a tandem of Scarce Sample Profiling and Next Generation RNA-seq. **Particular aims of the thesis are to:**

Uncover the differenced in deregulated actively translated transcripts between *in vitro* matured denuded & *in vivo* matured MII oocytes.

Investigate ART-relevant IVM conditions on the mouse model based on the IVM COC – IVO comparison

Set up IVF and assess BL developmental competency

Investigate the tandem of in vitro maturation & fertilization conditions on the IMZ – IVZ mouse PN zygotes

Investigate the relation between rFSH administration and global protein synthesis under ART-relevant conditions

3. Materials and Methods

Mice breeding & Oocyte Maturation

8-week-old female ICR mice bred in-house (12 hours day-night cycle) were stimulated with 5IU pregnant mare serum gonadotropin (PMSG) 46 hours before sacrifice by cervical dislocation. Fully grown germinal vesicle stage oocytes were harvested as IVM DO or IVM COC by ovum pick-up in 0,1% (v/v) isobutyl-methyl-xanthine (IBMX, ProSpec) supplemented transfer media. After washing in IBMX free transfer media, the collected DOs were transferred for *in vitro* maturation into aMEM (M0200, Merck) media supplemented with 4 g/l BioXtra BSA (A3311, Merck) with 280 mOsm/kg osmolality. COC maturation medium was additionally supplemented with 5 ng/ml rFSH (Gonal, Merck) and 5 ng/ml rhCG (Ovitrelle, Merck). MII oocytes with an extruded 1st polar body were collected after 10 hours of *in vitro* culture following nuclear envelope breakdown (NEBD).

8-week-old female ICR mice destined for *in vivo* oocyte collection were stimulated with 5IU pregnant mare serum gonadotropin (PMSG) 46 hours prior to the administration of 5 IU rhCG (Ovitrelle, Merck). *In vivo* oocytes (IVO) were collected from isolated ovaries by ovum pick-up 11 hours post rhCG application. Collected IVM COC and IVO oocytes were denuded prior to freezing by 15-min treatment in media supplemented with 20 µg/mL hyaluronidase (H3506, Merck) for 15 minutes followed by mechanical denudation. Samples designed for SSP profiling were incubated for 10 minutes in culture media supplemented with 0.1 g/l cycloheximide prior to freezing at -80°C.

Scarce Sample Profiling

Cycloheximide-treated samples (200 oocytes or zygotes/sample) collected in quadruplicates and stored at -80°C were subjected to SSP profiling (Masek *et al.*, 2020). All sample handling was performed on ice. Briefly, cells were lysed in 350 µl of polysome extraction buffer containing 1% (v/v) Triton X-100, RNAse inhibitor (Ribolock, Thermo), and protease inhibitor cocktail (Complete EDTA-free, Roche). To ensure complete disruption of the zona pellucida, zirconia-silica beads were added to tubes containing samples. Prepared samples were loaded into a mixer mill (MM301, Retsch GmbH) and shaken 3 times for 1 minute at 30 Hz with intermittent cooling on ice. Meanwhile, a sucrose gradient (10 – 50%) was prepared in SW55Ti tubes (Beckman Coulter) in a Gradient Master 108 ^{TM} (BioComp) from individual 10% and 50% sucrose solutions containing the same components as the lysis buffer, except for the Triton X-100. Sample lysates were cleared by centrifugation at 10 000x g, 4°C for 10 minutes. The supernatants were loaded onto the prepared sucrose gradients and subjected to ultracentrifugation at 45 000 RPM, 4°C for 65 minutes in an Optima L-90 ultracentrifuge (Beckman Coulter). The ultracentrifugation samples were then fractionated into 10 equal

fractions by pumping 60% sucrose solution into SW55Ti tubes with the fractionated samples. The absorbance of the outlet was continuously monitored with a UA-5 detector and UV absorbance reader (Teledyne, ISCO) to determine the beginning and the end of the fractionation process. The overall quality of polysome profiling was monitored by the parallel fractionation of HEK293 cell lysate. The fractionation profile itself was determined by qPCR.

RNA isolation & qPCR

Each fraction was collected into a 2-ml tube containing 1 µl of GenElute LPA (56575, Merck). Immediately after fractionation, 900 µl of TRI Reagent (T9424, Merck) was added into each tube followed by 3 minutes of vortexing, then 350 µl of chloroform was added and again vortexed vigorously for 3 minutes. After centrifugation for 10 minutes at 13 000 RPM, 4°C the upper phase was transferred into a new tube and mixed with an equal volume of 100% ice-cold isopropanol. After overnight precipitation at -20°C, samples were centrifuged for 40 minutes at 13 000 RPM, 4°C. The supernatant was removed, and the pellet was washed with 1 ml of 75% (v/v) ice-cold ethanol. Samples were vortexed briefly and centrifuged for 5 minutes at 13 000 RPM, 4°C. After repeated ethanol washes, the sample pellet was quickly air-dried and resuspended in 12 µl of RNAse-free water. 2 µl of isolated RNA were used for cDNA synthesis to backtrack polysome profiles.

cDNA was synthesized from total RNA with a qPCRBIO cDNA synthesis kit containing a mix of oligo dT and random primers (PCR Biosystems) according to the manufacturer's protocol. For 18S and 28S rRNA qPCR, 5 µl of LightCycler480® SYBR Green I Master mix (Roche) was mixed with 2 µL of cDNA and 2 µl of the respective 2,5uM gene-specific primer pair (Supp. Table 1) in a total reaction volume of 10 µl. Each reaction was performed in triplicates. For the absolute quantification, recombinant pCR™4-Topo™ plasmids (Invitrogen) containing 18S and 28S rRNA amplicons were prepared to calculate a standard curve.

Library preparation & RNA-Sequencing

Quadruplicate samples were pooled into non-polysomal (NP; fractions 1-5) and polysomal (P; fractions 6-10) samples, and accompanied by an unfractionated total RNA sample (T). RNA was dissolved in RNAse-free water at a minimal concentration of 250 pg total RNA per sample. Sample Quality Assessment was performed with a RNA 6000 Pico Chip (Agilent) using a Bioanalyzer 2100 instrument (Agilent). cDNA libraries were prepared with a SMARTer Stranded Total RNA-Seq Kit v2 Kit - Pico Input Mammalian (Takara Bio) according to the manufacturer's instructions. Library quantification was performed using a Qubit™ DNA HS Assay Kit (Thermo). To perform cDNA library QC, the pre-sequencing of libraries was done in an iSeq 100 (Illumina) with the following settings (number of reads: 4 million, 150 bp read length, base call quality > Q30). The NGS RNA-seq was done on NovaSeq 6000 (Illumina) in an S4 Flow Cell with the following settings

(number of reads/sample: 100 million; 150 bp read length, Paired End). The output sequencing data were in FASTQ format.

Bioinformatic Analysis

Reads were quality checked with FastQC (v. 0.11.9) followed by read alignment to the mouse genome (build GRCm39); transcript quantification and the detection of probable gene fusions was performed with the DRAGEN (Dynamic Read Analysis for GENomics) Bio-IT Platform (Illumina) RNA pipeline (3.7.5). Further RNA-Seq, PCA, DGE and GO analyses were performed with the software CLC Genomics Workbench 22.0.1 (Qiagen). Transcripts with a cutoff at 0.2 RPKM were considered for the DGE analysis.

Western Blot

MII oocytes and pronuclear embryos were lysed with 6 µl of ddH_2O and 2.5 µl of 4X NuPAGE Lysis buffer (NP007, Life-Technologies), and 1 µl reduction buffer (NP 0004, Thermo) at 100 °C for 5 minutes. Lysates were separated using a 4–12% gradient precast SDS-PAGE gels (NP323BOX, Life Technologies) and transferred to a PVDF membrane (Immobilon-P, Merck). The blotting was performed with a semidry system (TurboBlot, BioRad). Membranes were blocked for 1 hour in a blocking buffer (Azure Biosystems) or if required in 5% BSA diluted in Tween-Tris- buffer saline (TTBS, pH 7.4). Membranes were incubated at 4°C overnight in primary antibodies (Supp. Table 1) diluted at an optimized ratio. After the 3×10 min wash in TTBS buffer, membranes were incubated for 1 hour in a secondary antibody HRP peroxidase conjugated anti-rabbit produced in donkey (711-035-152, Jackson Immunoresearch) at 1:10 000 in TTBS for 1 hour at room temperature. The specific antibody signal was visualized by chemiluminescent ECL reagent (Amersham, Cytiva). Signal detection was performed on Azure 600 (Azure Biosystems). Signal quantification was done with AzureSpot software 2.1 (Azure Biosystems). Normalization between samples was done using GAPDH or α-Tubulin.

^{35}S-methionine Labelling

In order to determine *de novo* protein synthesis in MII oocytes and pronuclear zygotes cultured *in vitro* and *in vivo*, the ^{35}S-methionine incorporation assay was applied according to a previously published approach (Šušor *et al.*, 2008). Briefly, after maturation in the respective culture conditions, samples were denuded by treatment with 6 µg/ml hyaluronidase for 15 minutes if applicable and treated with 25 µCi/ml of ^{35}S-methionine (Hartmann analytics) for 1 hour. After incubation, samples were washed in polyvinylalcohol (PVA)-supplemented phosphate-buffered saline (PBS) and stored for Western blotting at -80°C. Following the SDS-PAGE Western blotting protocol as described above, samples were transferred to the PVDF membrane (Immobilon-P, Merck) by semidry transfer for 25 minutes at 5 mA/cm^2 (TurboBlot, BioRad). Blotted

radioactive samples were then exposed in a cassette with a FujiFilm autoradiographical membrane for 7 days. The signal was recorded with a BAS-2500 Photo Scanner (FujiFilm Life Sciences) and quantified with the software ImageJ. Normalization between samples was done using GAPDH.

Immunocytochemistry

For protein visualization, oocytes and embryos were fixed for 15 min in 4% PFA (Merck) in PBS. Fixed oocytes were permeabilized in 0.1% Triton X-100 for 10 min, washed in PBS supplemented with PVA (Merck) and then incubated with primary antibodies overnight at 4 °C (Supp. Table 1). Oocytes were then washed 3X for 15 minutes in PVA/PBS, and the detection of primary antibodies was performed using relevant Alexa Fluor 488 or 647 conjugates (Invitrogen) diluted 1:500 and incubated for 1 hour at room temperature. Washed oocytes (3 times 15 min in PVA/PBS) were subsequently mounted on a slide in Vectashield Mounting Medium containing DAPI (Vector Laboratories) and solidified for at least an hour prior to imaging on a confocal microscope (SP5, Leica). Images were processed with LasX software (Leica).

Gap-junctional Assay

Calcein-acetoxymethyl ester (AM) dye (56496, Merck) 1 mM-stock solution was freshly prepared in 0.1% DMSO. The respective matured oocytes were incubated in culture media with 1 µM Calcein-AM for 25 minutes to facilitate dye exchange between oocytes and cumulus cells and to allow time for the conversion of non-fluorescent Calcein-AM to fluorescent Calcein (permeable only via gap junctions) by intracellular esterases. After the incubation, oocytes were washed 3 times in transfer media and immediately imaged on the epi-fluorescent microscope (DMI 6000B, Leica) using a filter for green fluorescence.

Mitotracker Labelling

Matured oocytes were incubated in freshly prepared media (M0200, Merck) supplemented with 4 g/L BioXtra BSA (A3311, Merck) and 100 nM Mt-CMXRos for 30 minutes. After a quick wash in transfer medium (TM), oocytes were transferred into pre-warmed 4% paraformaldehyde and incubated at room temperature for 30 minutes. After three consecutive washes in PVA/PBS buffer, oocytes were mounted in Vectashield HardSet mounting medium with DAPI (Vector Laboratories) and hardened for 1 hour prior to imaging. Images were acquired in a TCS SP5 confocal microscope (Leica) with a DPSS 561 nm laser.

In Vitro Fertilization & blastocyst development

Motile sperm was collected from the cauda epididymis of 12-month-old ICR mouse males by needle puncture. Sperm capacitation for 1 hour as well as subsequent IVF was performed under IVF-grade paraffin oil (Vitrolife) in 100 µL of equilibrated HTF medium (Merck) supplemented with 4 g/L BioXtra BSA (A3311, Merck) and 1mM BioXtra GSH (G6529, Merck) 30 min before the IVF; matured MII oocytes were added into the HTF media. The IVF itself was performed by adding 4 µL of capacitated motile sperm to the HTF media containing IVM DO MII oocytes. After 4 hours of co-culture with capacitated sperm, zygotes were transferred into 100 µL of equilibrated fresh advanced KSOM medium (MR-101-D, Merck) under IVF grade paraffin oil (Vitrolife) for an additional 4 hours. Next, pronuclear zygotes with both maternal and paternal pronuclei present were selected and washed three times in transfer medium and once in PVA/PBS medium prior to freezing at -80°C.

Live Cell Imaging

Oocyte *in vitro* maturation and early embryo development was live-cell imaged (LCI) on epi-fluorescent microscope (DMI 6000B, Leica) in a controlled and humidified atmosphere at 37°C, 5% CO_2. LCI was performed in a 30 µL drop of respective media overlaid with 800 µL of an IVF-grade paraffin oil (Ovoil, Vitrolife) in a 4-well chamber (Sarstedt). The chamber with media and oil was preheated and equilibrated over 4 hours prior to introducing experimental samples. Oocytes and embryos were imaged every 10 minutes (bright-field imaging) or shortly before and after the first polar body extrusion under green fluorescence (SiR-tubulin, SC002, Spirochrome).

4. Results

4.1 Synchronization of in vitro and in vivo maturation

This project is based on in-house bred ICR mice, stimulated with pregnant mare serum gonadotropin (PMSG) to obtain fully matured germinal vesicle (GV) oocytes. These were either *in vitro* matured as denuded (IVM DO) or as cumulus-oocyte complexes (IVM COC) until the metaphase II (MII) stage (Fig. 7). *In vivo* maturation was triggered by simulating the luteinizing hormone (LH) surge with recombinant human chorionic gonadotropin (rhCG). *In vivo* MII oocytes (IVO) with expanded cumulus cells were mostly present at 14 hours post rhCG administration within the infundibular region of the fallopian tubes. To simulate conventional *in vitro* maturation technology in assisted reproduction more closely, we selected the αMEM as *in vitro* culture medium, i.e. containing free amino acids and vitamins in addition to M16. Initial observation has shown morphological difference related to cumulus cell expansion of cumulus-oocyte complexes matured *in vitro* in M16 or αMEM supplemented with rFSH, rhCG (Fig. 8).

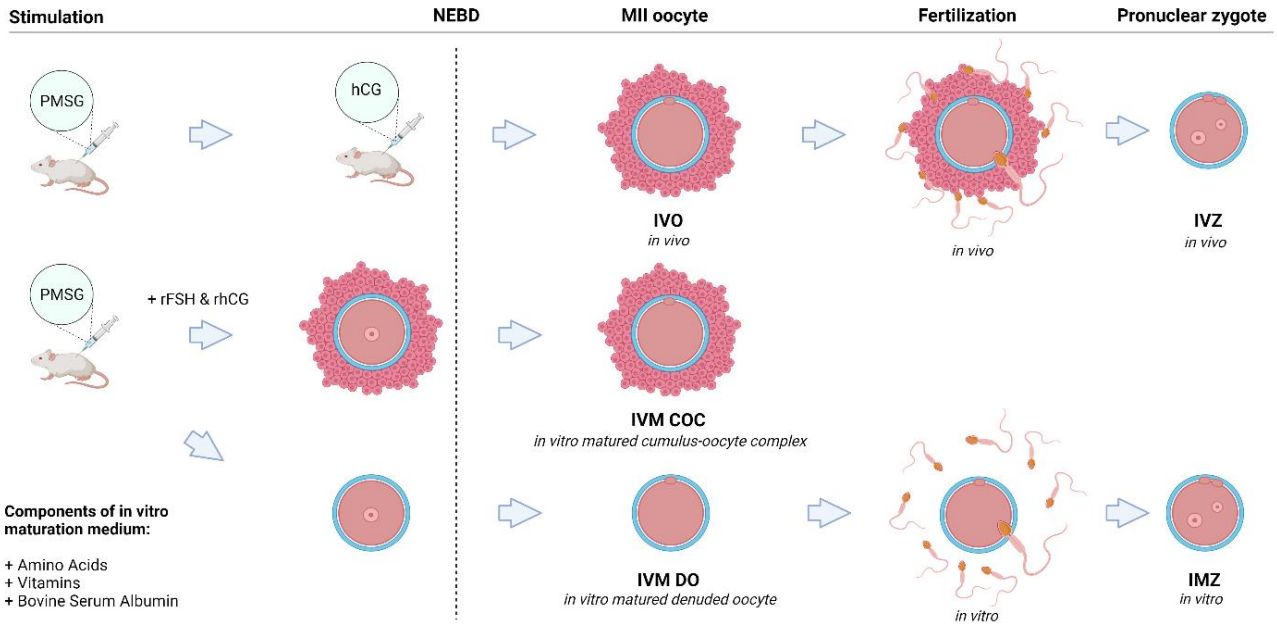

Fig. 7 The mouse model to study of clinically relevant *in vitro* and *in vivo* matured MII oocytes and pronuclear zygotes. The scheme of collected ICR mouse oocytes and zygotes for the SSP profiling and total transcriptome analysis. GV oocytes were matured *in vitro* to the MII stage as denuded (IVM DO) or as cumulus-oocyte complexes in the presence of rFSH and rhCG (IVM COC). Pronuclear zygotes were generated by *in vitro* fertilization (IVF) of IVM DO (IMZ) or by rhCG administration and male mating followed by collection of *in vivo* zygotes (IVZ). (Created with BioRender.com)

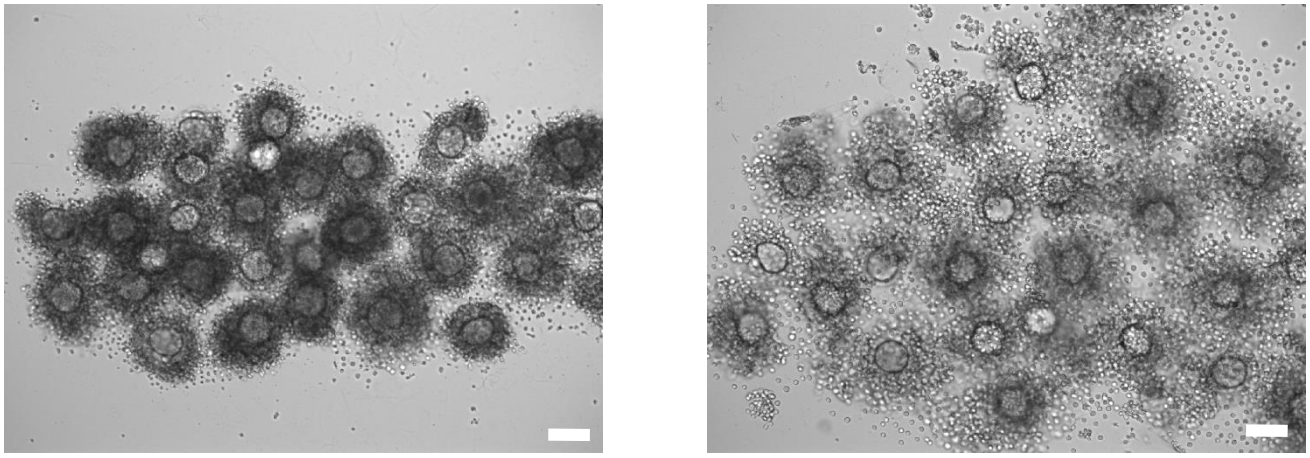

Fig. 8 Different morphological appearance of *in vitro* matured cumulus-oocyte complexes. *In vitro* matured cumulus-oocyte complexes in M16 medium (left) and αMEM medium (right), both supplemented with rFSH and rhCG. Scale bar = 100 µm

As already mentioned, to achieve the fertilization potential and developmental competence, the oocyte has to complete both nuclear and cytoplasmic maturation. Nuclear maturation is completed upon proper MII spindle formation, in contrast to loosely defined cytoplasmic maturation. We observed a delay between the 1st PBE and completion of nuclear maturation by the Live-Cell Imaging of sir-tubulin labelled *in vitro* matured denuded MII oocytes (IVM DO) (Fig. 9). As the 1st PBE of *in vitro* meiotic maturation is happening around 8 hours post nuclear envelope breakdown (NEBD), the IVM DO sampling time was set to 10 hours post NEBD to accommodate the time needed for spindle formation.

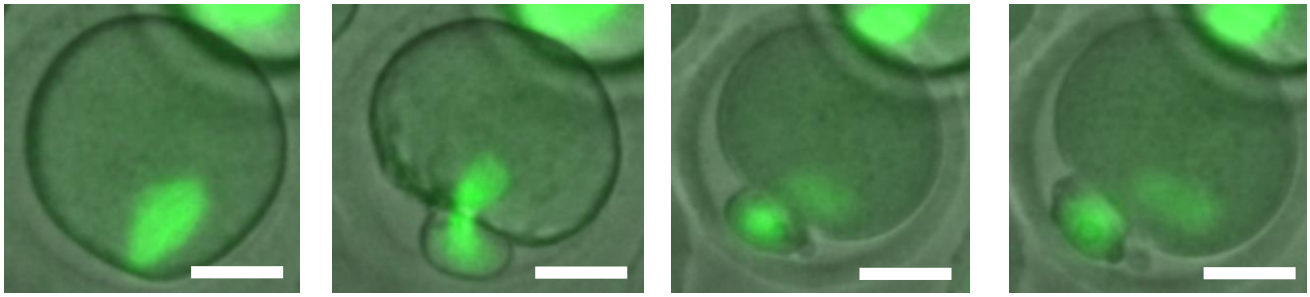

Fig. 9 The completion of nuclear maturation of *in vitro* matured oocytes is delayed respective to the morphological appearance of the 1st polar body. Live Cell Imaging of sir-tubulin labelled spindle (green) within *in vitro* matured denuded oocytes (bright-field). From left to right, images of the 1st polar body extrusion and MII spindle formation were taken in 30 minutes intervals. Scale bar = 30 µm

Setting up *in vivo* oocyte maturation sampling to reflect in vitro timing was challenging. As we wanted to simulate conditions in assisted reproduction technology (ART), we set the sampling towards the key point in the clinical ovarian hyperstimulation protocol, the ovum pick up (OPU). The OPU is commonly done in patients shortly before ovulation, which corresponds to around 11 hours post rhCG administration in mice (Fig. 10). At this time cumulus-oocyte complexes (COCs) are expanded, follicle wall is translucent and vascularized. All this is signalling that follicles are about to ovulate. Based on the data obtained by the

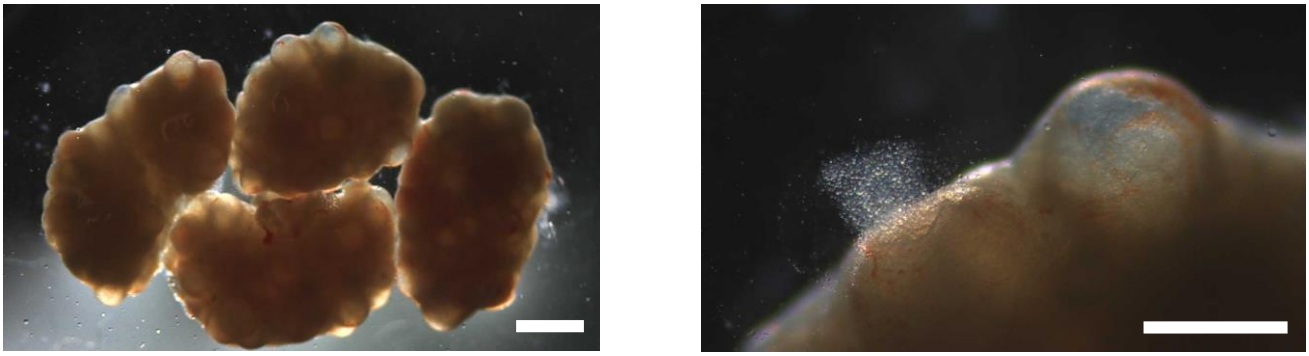

Fig. 10 *In vivo* oocyte meiotic maturation within mouse ovarian follicles. Bright-field images of wild-type mouse ovaries retrieved 11 hours post subcutaneous injection of rhCG into a mammary fat pad, scale bar = 3 mm; a detail on a ready-to ovulate follicle and a needle-pricked follicle containing an expanded COC, scale bar = 1 mm

immunocytochemical staining of acetylated tubulin, about 80-90 % of collected *in vivo* MII oocytes had completed nuclear maturation (Fig. 11). The remainder was still in the process of maturation. These data suggested that prolonged *in vivo* incubation time within oviducts led to rapid post-ovulatory aging accompanied by progressive spindle destabilization (Fig. 11, 12), which was gradually increasing from 16 hours post rhCG administration onwards.

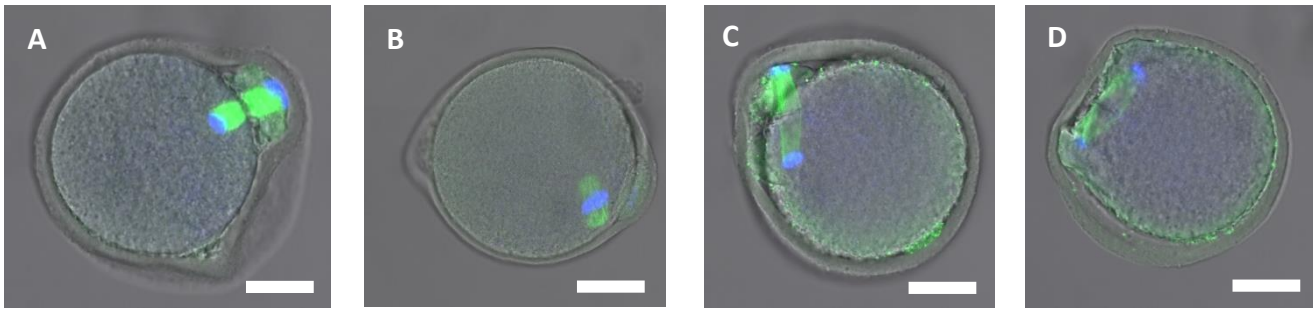

Fig. 11 Spindle morphokinetics of *in vivo* matured MII mouse oocytes. Localization of acetylated tubulin (green), DAPI stained chromosomes (blue) within *in vivo* matured ICR mouse MII oocytes (bright-field); oocytes were retrieved as cumulus-oocyte complexes, fixed in paraformaldehyde and denuded by hyaluronidase treatment; MII oocytes in the process of MII spindle formation were classified as dynamic (A); oocytes with properly formed MII spindle were classified as matured (B); MII oocytes with loosening spindle equatorial plain were classified as aging (C); MII oocytes with spindle having anaphase-like morphology (D); scale bar = 30 µm.

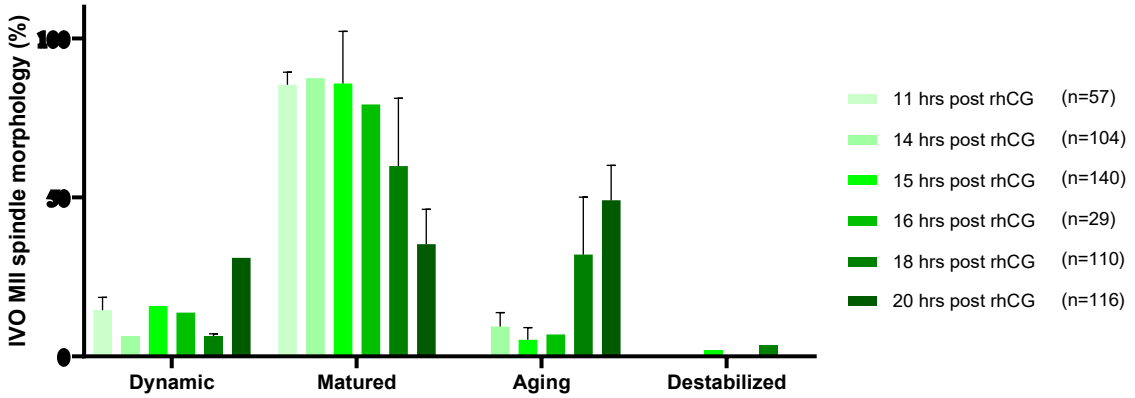

Fig. 12 Distribution of *in vivo* maturated MII mouse oocytes according to changing spindle stability. Analyzed data from immunocytochemical staining of *in vivo* matured, paraformaldehyde fixed and hyaluronidase denuded MII oocytes. Observed spindle morphology is classified as dynamic, matured, aging and destabilized. Data are presented as the mean±s.d.; from two independent experiments, $n \geq 29$

Further experiments confirmed the occurrence of *in vivo* NEBD. As the occurrence of NEBD *in vivo* is dependent on the luteinizing hormone (LH) surge, the initial observation of the amphiregulin, a downstream effector of LH receptor, expression was performed in *in vivo* COCs (Fig. 13A). As expected, amphiregulin expression increased linearly with the greatest increment around 3-4 hours post rhCG adminstration. However, to pinpoint the actual NEBD phenotype, a simple bright-field morphological assessment of *in vivo* matured oocytes was also done (Fig. 14). This confirmed the occurrence of *in vivo* NEBD at around 3 hours post rhCG adminstration. Together with previous results, the *in vivo* maturation time from NEBD to an Egg can be estimated to about 8 hours *in vivo*.

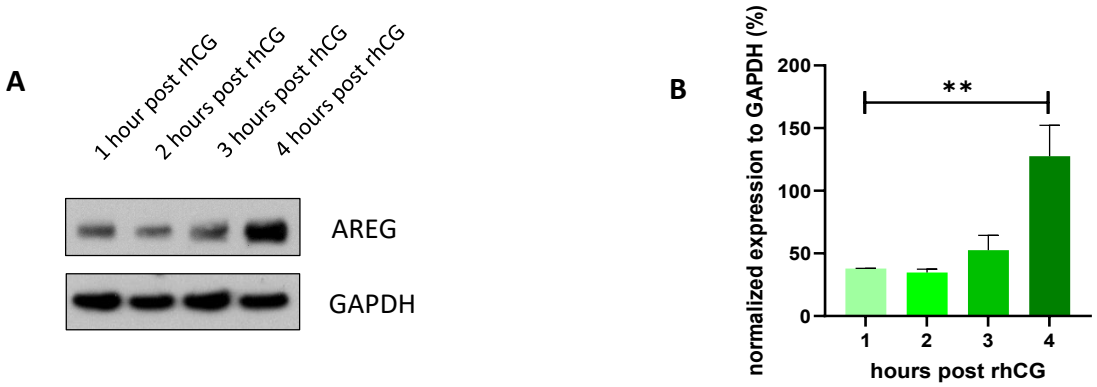

Fig. 13 Amphiregulin expression is increasing within cumulus-oocyte complexes upon rhCG administration *in vivo*. Western Blot data normalized to GAPDH showed rapid increase of Amphiregulin (AREG) expression (A) within mouse cumulus-oocyte complexes (A); signal quantification revealed greatest increase between 3 – 4 hours post rhCG administration (B). Data are presented as the mean±s.d.; **P<0.01 according to one-way ANOVA; two independent experiments.

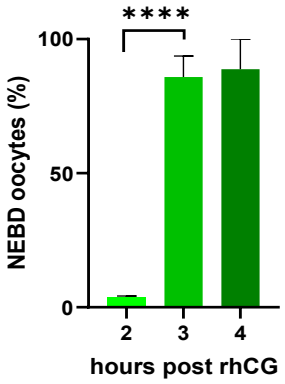

Fig. 14 Nuclear envelope breakdown occurs within hours post rhCG administration *in vivo*. Morphological assessment of germinal vesicle and nuclear envelope breakdown (NEBD) oocytes at 2-4 hours post rhCG administration revealed that the majority of oocytes undergo NEBD at 3 hours. Data are presented as the mean±s.d.; ****P<0.0001 according to Student's *t*-test; three independent experiments, *n* ≥35.

As *in vivo* matured oocytes (IVO) are enclosed by cumulus cells during meiosis, we wanted to investigate to what extent the communication via trans-zonal projections (TZPs) is active and when it ceases. To do that, a gap junctional assay was employed, which is based on conversion of permeable non-fluorescent Calcein-AM

by esterases cleavage within oocyte's cytoplasm to non-permeable fluorescent Calcein. The gap-junctional assay results confirmed the closure of TZPs by consistent increase of fluorescent Calcein signal intensity within oocyte's cytoplasm at 10 and 20 hours post rhCG administration. Collected and denuded *in vivo* oocytes at 0 hours post rhCG administration served as a control, where all TZPs are closed. At 5 hours post hCG administration, no signal within oocyte's cytoplasm was observed (Fig. 15).

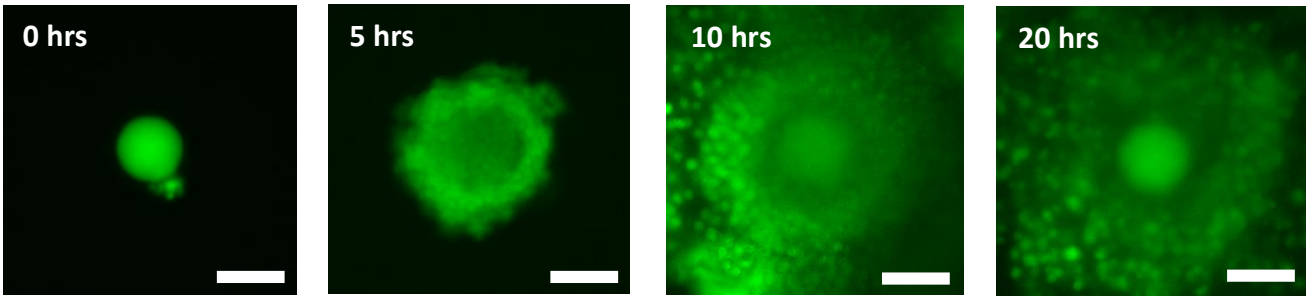

Fig. 15 Oocyte – cumulus communication cease half-way through meiotic maturation *in vivo*. Fluorescent images of Calcein-AM treated *in vivo* matured cumulus-oocyte complexes at various timepoints post rhCG administration. The 0 hour treatment was performed on a denuded oocyte and served as a control for dye accummulation within the cytoplasm, scale bar = 80 µm.

4.2 Cumulus-Oocyte complex *In Vitro* Maturation

The most relevant group for our comparison with IVO respective to ART are in vitro matured cumulus-oocyte complexes (IVM COC). These are isolated upon OPU and in vitro matured in the amino acids rich media with the presence of rFSH and rLH or rhGC. Initially, the GV maturity assessment of collected IVM COC was done in order to ensure that we are able to discern morphologically the matured surrounded nucleolus (SN) from immature non-surrounded nucleolus (NSN) configuration. Simple immunocytochemical staining of chromatin by 4',6-diamidino-2-phenylindole (DAPI) combined with bright-field imaging confirmed our ability to selectively collect only SN IVM COCs (Fig. 16). Further, the IVM COC culture media composition was defined to be similar to the media conventionally utilized by ART clinics.

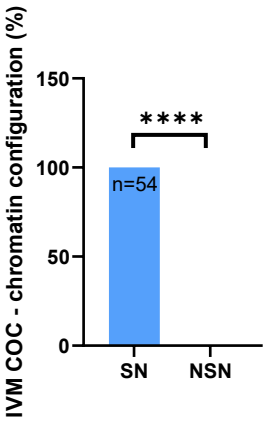

Fig. 16 Collected cumulus-oocyte complexes utilized for *in vitro* maturation possessed exclusively matured surrounded nucleolus configuration. Morphological assessment of germinal vesicle and nuclear envelope breakdown (NEBD) oocytes at 2-4 hours post rhCG administration revealed that the majority of oocytes undergo NEBD at 3 hours. Data are presented as the mean±s.d., ****P<0.0001, according to Student's *t*-test; from two independent experiments, *n*≥29.

Selected αMEM medium supplemented with amino acids, bovine serum albumin and rFSH, rhCG was tested for its ability to support cumulus expansion and oocyte meiotic maturation. As we were able to visually detect the point of NEBD and 1st PBE within IVM COCs by Live Cell Imaging, the timing from IBMX release to NEBD and 1st PBE was recorded. Acquired results showed a significant delay in NEBD of IVM COC group compared to IVM DO group, however, regarding the time from NEBD to 1st PBE, IVM COCs were maturing faster. Together, the overall maturation time from IBMX release to 1st PBE was very similar (Fig. 17).

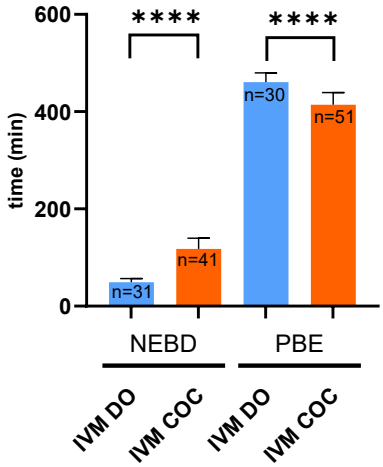

Fig. 17 The overall *in vitro* maturation time is similar between denuded and cumulus-enclosed oocytes. In vitro matured denuded oocytes (IVM DO) and in vitro matured cumulus-oocyte complexes (IVM COC) varied in timing between IBMX release-NEBD (around 60 min) and NEBD-1st PBE (around 50 min). The overall IBMX release-1st PBE maturation time was highly similar. Data are presented as the mean±s.d.; ****P<0.0001, according to Student's *t*-test; from three independent experiments, *n*≥30

To evaluate the probable benefit of cumulus cells presence for in vitro maturation, we first investigated the cumulus expansion. The very first observation of IVM COC behaviour upon media selection (Fig. 8) showed greater cumulus cell expansion in αMEM rather than M16 media. The main difference between them is the presence of amino acids and vitamins in the former one. Even though αMEM has improved the cumulus expansion, it did not form as solid bulk of cumulus cells surrounded oocyte as was the case for IVO cumulus cells. Therefore, an additional experiment with IVM COC cultured in ART defined αMEM media with or without further supplementation of 10 % foetal bovine serum (FBS) was performed. Live Cell Images have shown more similar structure to IVO with serum supplementation than without (Fig. 18).

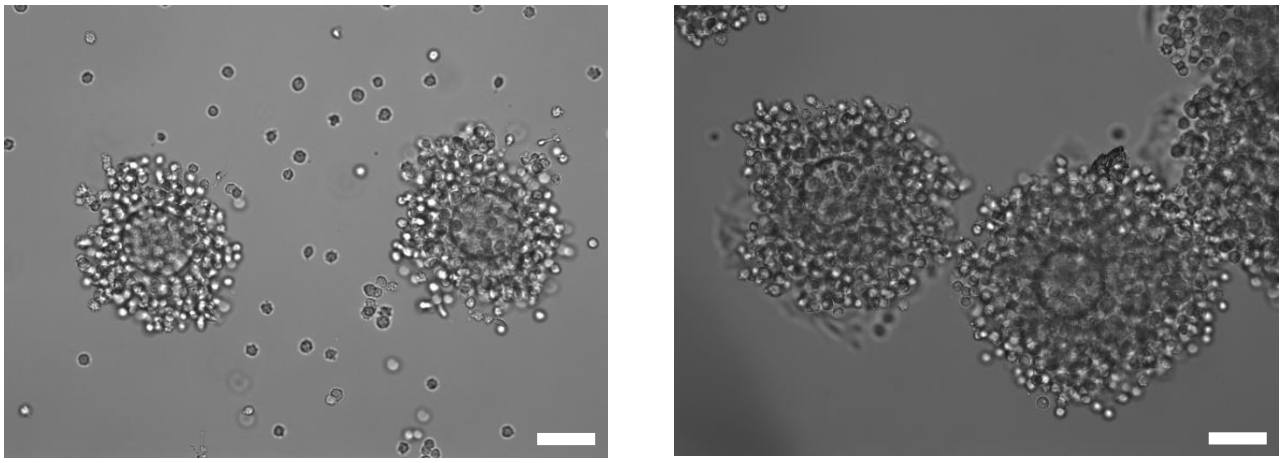

Fig. 18 The addition of foetal bovine serum greatly enhanced the structure of *in vitro* matured cumulus-oocyte complex. Bright-field images of *in vitro* matured cumulus-oocyte complexes in αMEM medium, supplemented with recombinant FSH, recombinant hCG, and either bovine serum albumin (left) or foetal bovine serum (right). Scale bar = 80 µm.

4.3 In Vitro Fertilization

In vitro fertilization (IVF) was essential to confirm the developmental competence of our *in vitro* matured oocytes as well as production of *in vitro* fertilized IVM DO pronuclear zygotes. After few initial unsuccessful experiments it was determined that the key for a successful IVF is appropriate handling and adequate medium supplementation for both matured oocytes as well as capacitated sperm. Moreover, an IVF grade paraffin oil was used exclusively for all IVF steps performed under oil. The initial results tested IVO group as a control of the IVF protocol efficiency. In addition, the difference between standard BSA or 10% FBS supplementation during IVM COC maturation was evaluated by the IVF made blastocysts (Fig. 19).

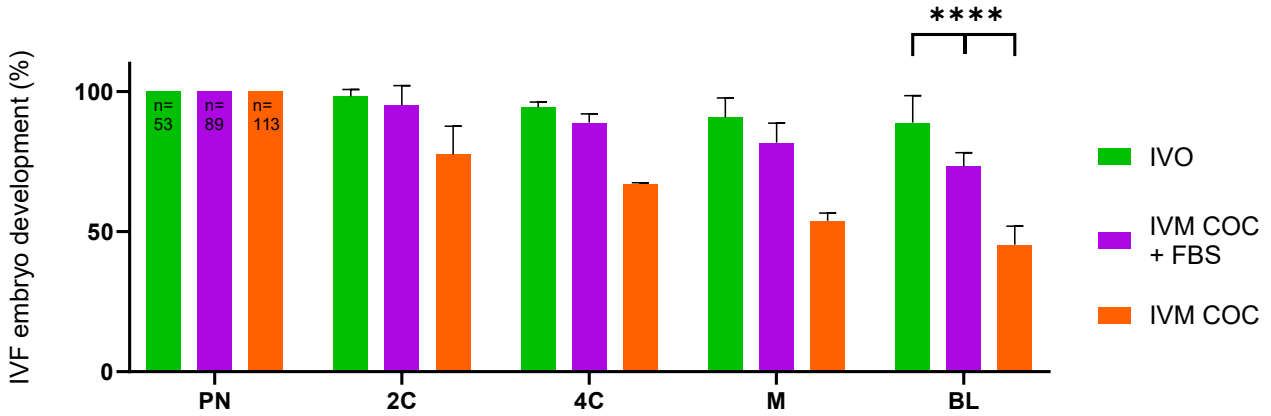

Fig. 19 Serum supplementation increases developmental potential of in vitro fertilized *in vitro* matured cumulus-oocyte complex. In vivo matured and in vitro matured cumulus-oocyte complexes in presence or absence of foetal bovine serum were subjected to in vitro fertilization. Serum supplementation greatly increased blastocyst rates in comparison with only bovine serum albumin. Data are presented as the mean±s.d.; ****P<0.0001, according to two-way ANOVA; from three independent experiments, *n*≥53

4.4 Pronuclear zygote collection

After mastering the IVF technique, *in vitro* pronuclear zygotes (IMZ) were produced by IVF of IVM DO. In parallel, pronuclear zygotes matured and fertilized *in vivo* (IVZ), were collected. However, IMZ and IVZ timing had to be synchronized just as previously collected oocytes, to compare only the effect of culture conditions and not any difference between developmental stages. IVM DOs undergone IVF at 14 hours post NEBD and developed to IMZ within 8 hours. The IVZ were collected at 20 hours post rhCG administration, which was coupled with overnight mating. IMZ and IVZ pronuclear zygotes were highly similar at defined collection time (Fig. 20).

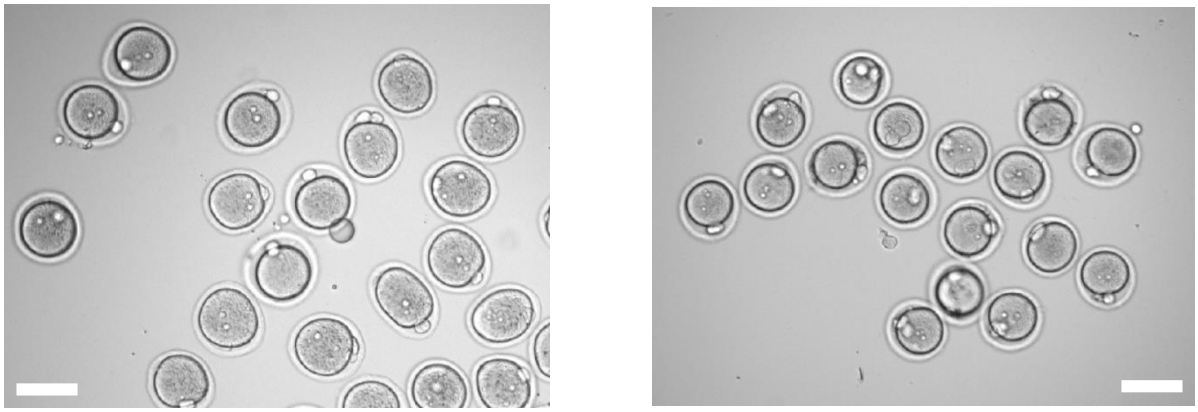

Fig. 20 *In vitro* and *in vivo* produced pronuclear zygotes show similar morphology. Bright-field images of pronuclear zygotes that resulted from *in vitro* fertilized *in vitro* matured denuded oocytes (left) and *in vivo* collected pronuclear zygotes (right) collected at 8 hours from the beginning of *in vitro* fertilization and 20 hours post recombinant human chorionic gonadotropin administration, respectively; scale bar = 80 µm.

Nevertheless, IVZ fertilization was obscured and vaguely defined, an approximate fertilization time was established based on the assumption that if ovulation takes place at 12 hours post rhGC administration *in vivo*, fertilization cannot happen earlier than one hour later, i.e. 13 hours. The opposite fixed point detectable by Live Cell Imaging was the NEBD of zygotic pronuclei. Acquired experimental data from Live Cell Imaging confirmed no difference between IMZ and IVZ with respect to set collection timing (Fig. 21).

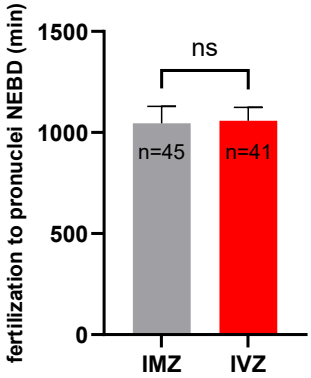

Fig. 21 Timing of post-fertilization zygote development between *in vitro* and *in vivo* produced pronuclear zygotes is similar. Data from bright-field Live Cell Imaging of *in vitro* fertilized *in vitro* matured denuded oocytes and *in vivo* matured and fertilized oocytes were assessed against the point of pronuclear NEBD. Data are presented as the mean±s.d.; *ns*, non-significant, according to Student's *t*-test; from two independent experiments, $n \geq 46$.

4.5 Polysome Fractionation and sample preparation for RNA-seq

During the process of oocyte meiotic maturation and early embryo development, transcription is ceased, and translation predominates. Its proper regulation is vital for gametes to achieve developmental competency. To isolate transcripts bound by ribosomes, i.e. involved in translation, we utilized polysome fractionation. Hereinabove mentioned IVM DO, IVM COC, IVO, IMZ and IVZ samples were processed by the Scarce Sample Profiling method (SSP, Masek 2020). Initial experiment comparing polysome fractionation with and without the presence of ethylenediaminetetraacetic acid (EDTA) was performed. EDTA dissociates ribosomes from mRNA and therefore it serves as a control experiment showing disassociated polysomes. Due to the very low amount of input material, polysome profile was not detected by sole absorbance reading. It had to be reconstituted by cDNA synthesis of fractionated RNA and further qPCR analysis. Data from 18S rRNA qPCR, which is an integral part of the large ribosomal unit, showed with EDTA treatment progressive shift towards the first three fractions with almost none present in the polysomal part in the second half of the profile. Fractions containing 18S rRNA without EDTA showed normal polysomal profile (Fig. 22)

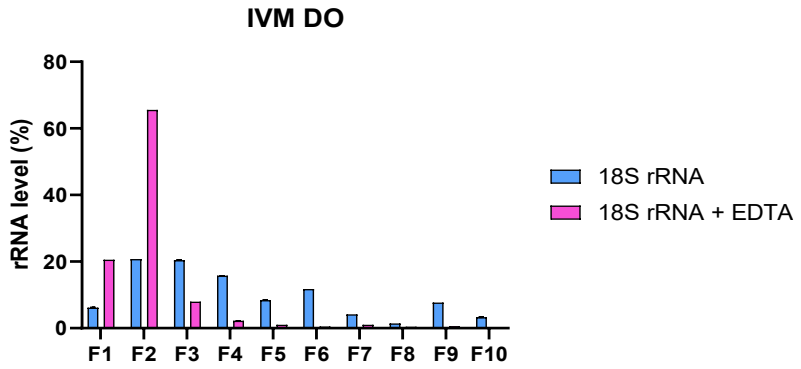

Fig. 22 The absence of polysome bound transcripts shifts fractionation profile towards the first half of collected fractions. In vitro matured denuded MII oocyte sample was processed by the Scarce Sample Profiling in the presence (pink) or absence (blue) of ethylenediaminetetraacetic acid. The sample was fractionated into 10 distinct fractions and qPCR of 18S rRNA was performed. Ethylenediaminetetraacetic acid treated fractionation process disassociated ribosomes from RNA and shifted the profile towards fractions 1-4. Data are presented as the mean±s.d.; from three technical replicates.

Following the initial process of validation with EDTA (Fig. 22), IVM DO, IVM COC, IVO, IMZ and IVZ samples were collected in quadruplicates for polysome fractionation. Isolated total RNA from fractions 1-5 was pooled together and named as non-polysomal. Isolated total RNA from fractions 6-10 was pooled together and named as polysomal. The pooling was done according to the reconstituted polysomal profile by qPCR of 18S rRNA and 28S rRNA (Fig. 23). Respective unfractionated total RNA was also isolated. Collected samples were used for cDNA library preparation and RNA-seq.

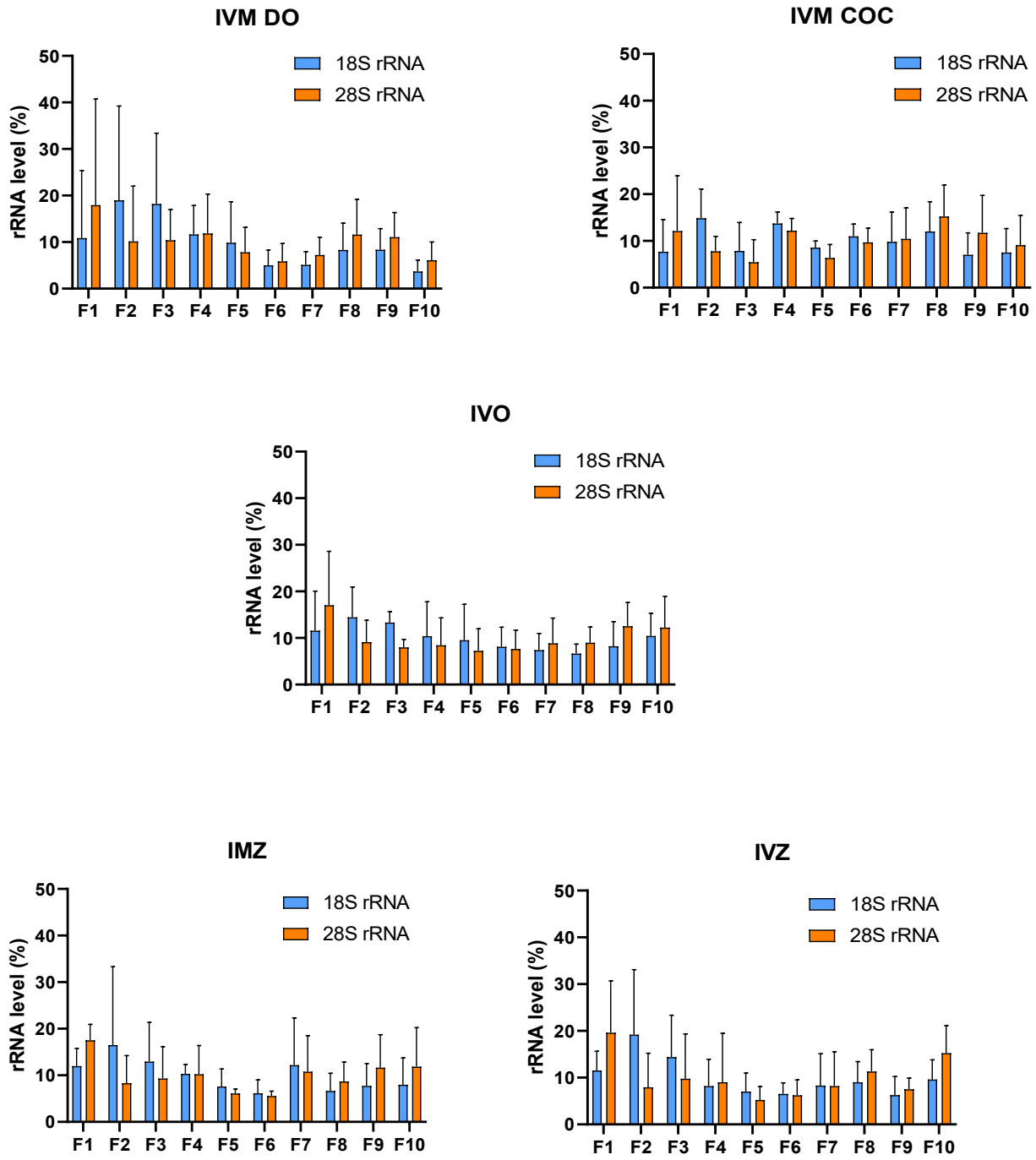

Fig. 23 Validation of the polysomal and non-polysomal distribution in fractionated samples. *In vitro* matured denuded oocytes (IVM DO), *in vitro* matured cumulus-oocyte complexes (IVM COC), *in vivo* matured oocytes (IVO), *in vitro* matured *in vitro* fertilized pronuclear zygotes (IMZ) and in vivo zygotes (IVZ) were subjected to Scarce Sample Profiling and qPCR of 18S rRNA (blue) and 28S rRNA (orange). The presence of polysomal and non-polysomal fractions as well as no EDTA pattern were observed. Presented as mean ± s.d.; from four independent experiments.

4.6 RNA-seq analysis and acquision of differentially expressed transcripts

SSP-fractionated RNA and total RNA samples were sent for RNA-sequencing to a company. RNA quantity was measured and cDNA library was prepared for every sample. Pre-sequencing was performed as additional control of produced libraries. Eventually, submitted samples went on for the Next Generation RNA-sequencing and both raw sequencing data as well as data mapped to a mouse genome GRCm39 were produced. Upon data retrieval, principal component analysis was made, which unravelled different clustering of polysomal and non-polysomal samples with respect to total transcriptome. Polysomal and non-polysomal samples of IVM DO, IVM COC and IVO also clustered differently, however, this was not the case for IMZ and IVZ samples (Fig. 24).

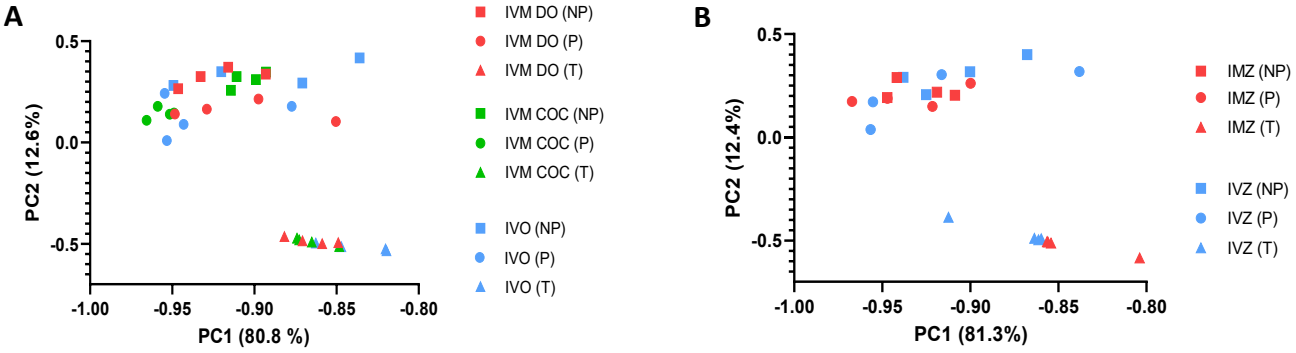

Fig. 24 Principal component analysis did not reveal clear difference among *in vitro* and *in vivo* SSP-fractionated samples, but showed clear difference in clustering with respect to total transcript. PCA analysis of mRNA transcripts mapped against GRCm39 mouse genome reference from *in vitro* matured denuded MII oocytes (IVM DO), *in vitro* matured cumulus-enclosed MII oocytes (IVM COC) and *in vivo* oocytes (IVO) (A); PCA analysis of mRNA transcripts mapped against GRCm39 mouse genome reference from pronuclear zygotes *in vitro* fertilized IVM DO (IMZ) and *in vivo* pronuclear zygotes (IVZ) (B); Analyzed RNA-seq data were sequenced from pooled non-polysomal fractions (NP), polysomal fractions (P) and total transcriptome (T). PCA analysis was performed by the GraphPad Prism software (9.5.1).

Further analysis processed mapped RNA-seq data and retrieved respective normalized valued for transcripts present in the dataset in a form of normalized reads per kiloblase million (RPKM) values. Differential gene expression (DGE) analysis was performed to compare *in vitro* and *in vivo* maturation conditions. Of particular interest was the comparison between polysomal and total fractions. The most obvious results were detected between IVM DO – IVO and IVM COC – IVO (Fig. 25). However, total transcriptome did not reflect these changes. IVM DO – IVM COC comparison on polysomal level showed however only very few transcripts displaying greater than 2-fold change. In this case, the pattern seen on polysomal level was reflected in total transcriptome. Similar global DGE trend as seen in IVM COC – IVO was observed between IMZ - IVZ dataset (Fig. 25).

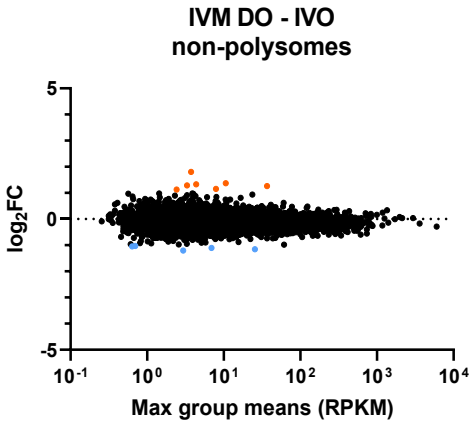
IVM DO - IVO
non-polysomes
log2FC
5
0
-5
10-1
100
101
102
103
104
Max group means (RPKM)

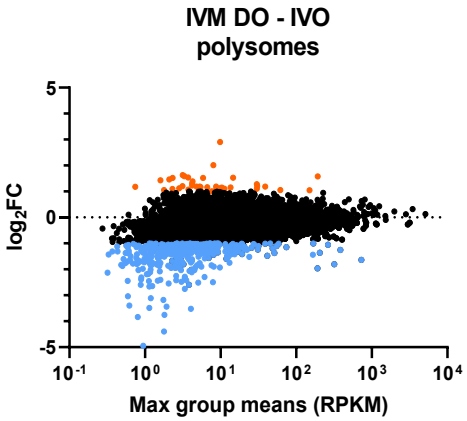
IVM DO - IVO
polysomes
log2FC
5
0
-5
10-1
100
101
102
103
104
Max group means (RPKM)

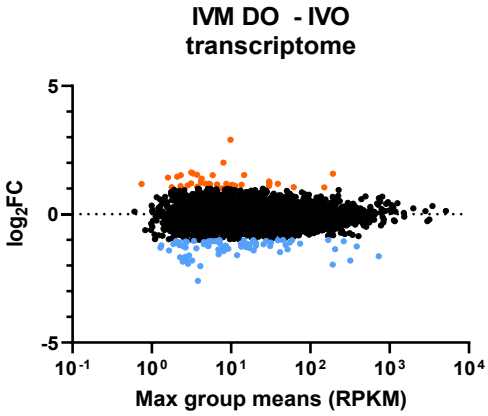
IVM DO - IVO
transcriptome
log2FC
5
0
-5
10-1
100
101
102
103
104
Max group means (RPKM)

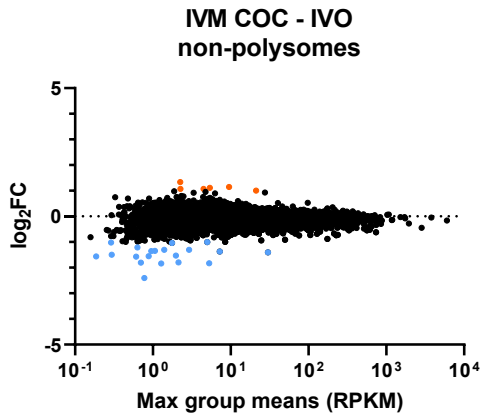
IVM COC - IVO
non-polysomes
log2FC
5
0
-5
10-1
100
101
102
103
104
Max group means (RPKM)

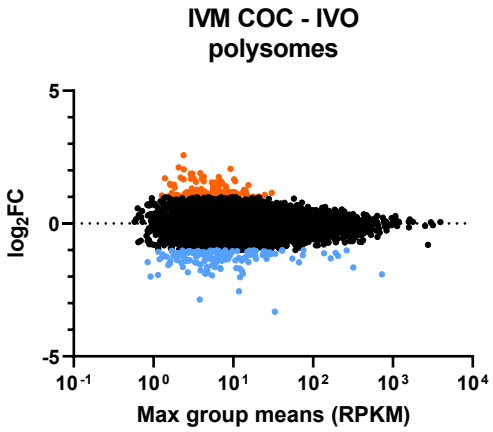
IVM COC - IVO
polysomes
log2FC
5
0
-5
10-1
100
101
102
103
104
Max group means (RPKM)

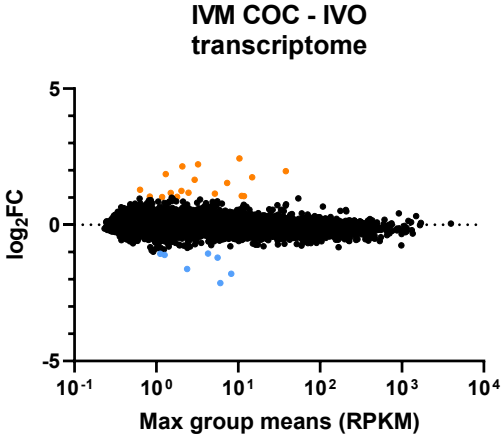
IVM COC - IVO
transcriptome
log2FC
5
0
-5
10-1
100
101
102
103
104
Max group means (RPKM)

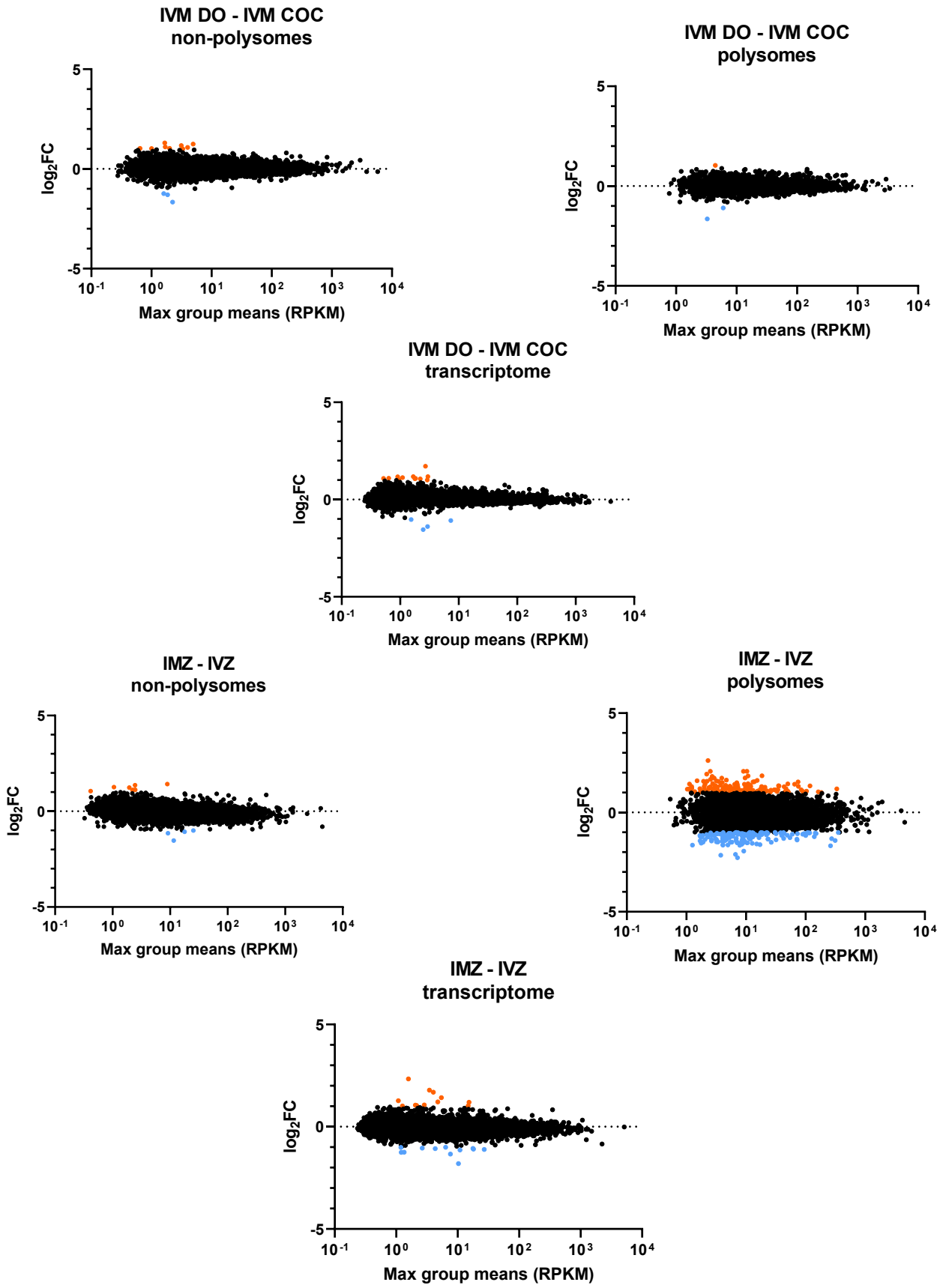

Fig. 25 Comparison of global translatome and transcriptome revealed differences between *in vitro* and *in vivo* conditions in both oocytes and zygotes. Differential expression analysis of mRNA from non-polysomal and polysomal fractions of SSP-profiles and total transcriptomes between *in vitro* denuded oocytes (IVM DO) and *in vivo* oocytes (IVO); *in vitro* cumulus-enclosed oocytes (IVM COC) and *in vivo* oocytes; *in vitro* denuded oocytes and *in vitro* cumulus-enclosed oocytes; *in vitro* fertilized IVM DO pronuclear zygotes (IMZ) and *in vivo* fertilized IVO pronuclear zygotes (IVZ). Max group means (RPKM >= 0.2) vs. $\log_2$ fold change ($\log_2$FC) (>=1) from RNA-seq data analysis.

Further gene-ontology enrichment analysis (GOEA) grouped actively translated DGE transcripts according to the related biological processes. Most deregulated biological processes were found between the IVM COC - IVO DGE transcripts. These processes were related to cell cycle regulation, chromosome organization, energy production, DNA repair or protein synthesis. The significance of biological processes clustering in IVM DO-IVO was greatest in energy production and chromosome organization related transcripts. The GOEA for the comparison between IVM DO-IVM COC forwarded the protein synthesis as the most significant biological process (Fig. 26). In the case of pronuclear zygotes, GOEA of IMZ-IVZ enhanced biological processes related to the cell cycle or RNA metabolism. Fewer DGE transcripts were related to microtubule organization or spindle assembly checkpoint (Fig 26).

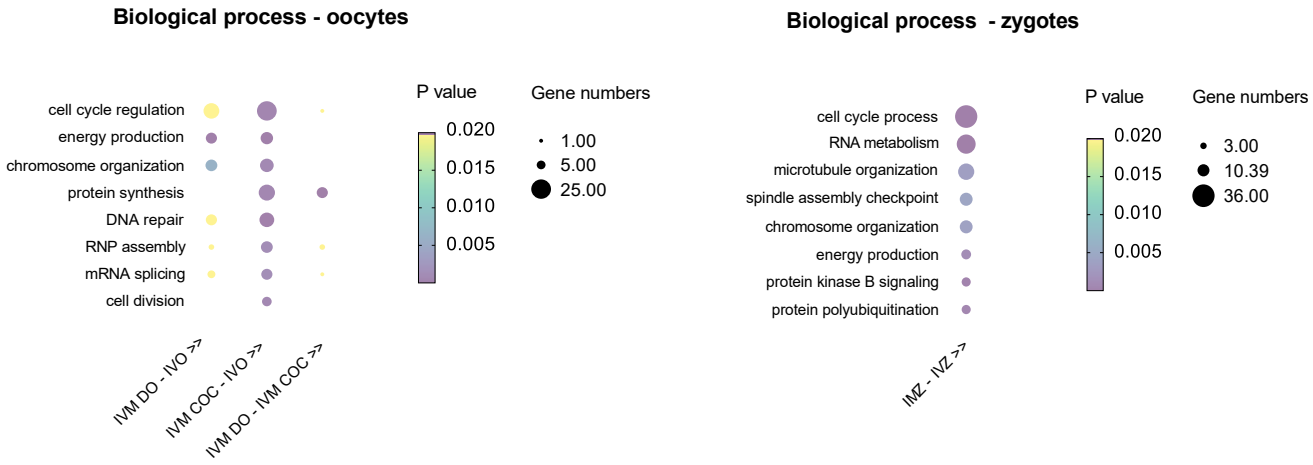

Fig. 26 Differentially expressed transcripts are deregulated in the cell cycle regulation, energy production or RNA metabolism. Gene ontology enrichment analysis performed between (IVM DO) and *in vivo* oocytes (IVO); *in vitro* cumulus-enclosed oocytes (IVM COC) and *in vivo* oocytes; *in vitro* denuded oocytes and *in vitro* cumulus-enclosed oocytes; *in vitro* fertilized IVM DO pronuclear zygotes (IMZ) and *in vivo* fertilized IVO pronuclear zygotes (IVZ), grouped differentially expressed transcripts according to biological processes involved mainly in cell cycle regulation, energy production, chromosome organization or protein synthesis. (Supp. Table 2)

4.7 Data validation

RNA-seq data were validated on multiple levels. At the individual transcript level, Western Blotting was selected. On higher level, changes in global translation were monitored by ^{35}S-methionine incorporation. To confirm changes in energy production, immunocytochemical approach was adopted.

Selected candidate transcripts*, Aurka, Cenp-V, Nsun2, Parn and others* were validated by Western Blot, as these „actively translated“ transcripts should reflect their changes in translation. DGE transcripts involved in the cell cycle regulation, *Aurka* and *Cenp-V,* were in comparison to IVO upregulated in IVM COC

and downregulated in IVM DO on protein level, respectively (Fig. 27). Pronuclear zygote related DGE transcripts involved in the RNA metabolism, *Nsun2* and *Parn,* were in both in comparison with IVZ downregulated on protein level in IMZ (Fig. 28).

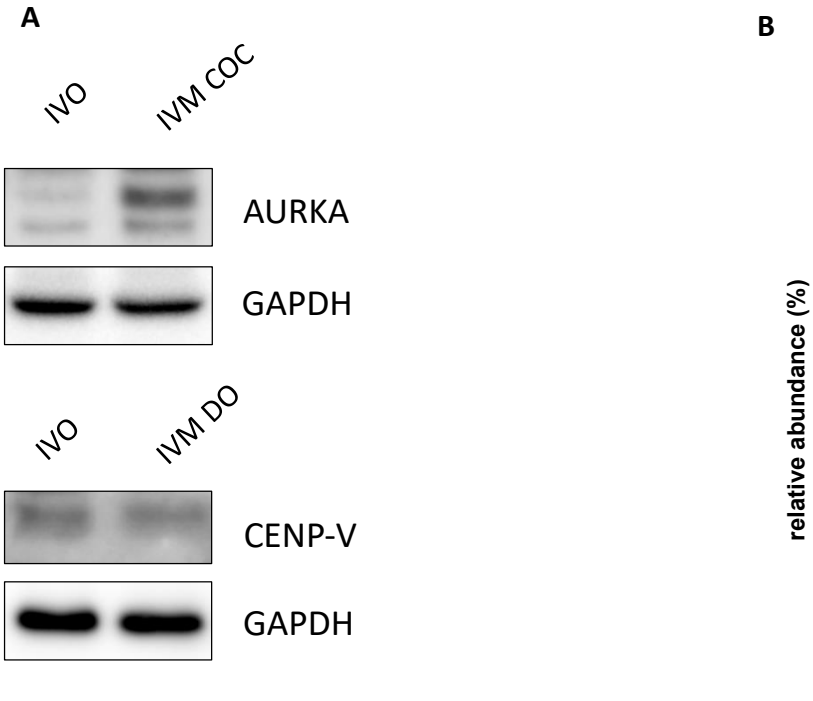

Fig. 27 Western Blot data and quantification of differentially expressed transcripts employed in the cell cycle regulation. Western Blot (A) and signal quantification (B) performed on AURKA in *in vitro* matured cumulus-oocyte complexes (IVM COC) and *in vivo* oocytes (IVO); and CENP-V protein in *in vitro* matured denuded oocytes (IVM DO) and *in vivo* oocytes (IVO); Data are presented as the mean±s.d.; *P<0.1; **P<0.01 according to Student's *t*-test; from at least three independent experiments.

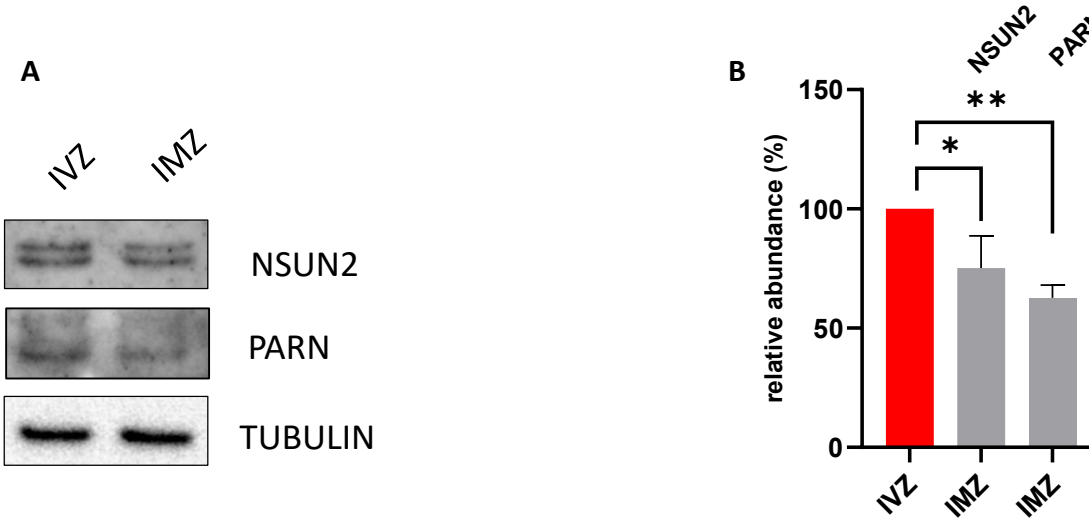

Fig. 28 Western Blot quantification of differentially expressed transcripts. Western Blot (A) and signal quantification (B) performed on NSUN2 and PARN in *in vitro* fertilized IVM DO pronuclear zygotes (IMZ) and *in vivo* fertilized IVO pronuclear zygotes (IVZ) Data are presented as the mean±s.d.; *P<0.1, **P<0.01 according to Student's *t*-test; from three independent experiments.

To validate the differences in global protein synthesis, the assay utilizing incorporation of ^{35}S labelled radioactive methionine was employed. Obtained results have shown a decrease in global protein synthesis of IVM DO and IVM COC with respect to IVO (Fig. 29A). However, no such difference was observed between IMZ and IVZ (Fig. 29B). It is worth mentioning that initial adopted protocol for 35S methionine labelling did not provide satisfactory results for further analysis as it was strongly dependent on media composition (Fig. 29C) in which the assay was performed. The issue was resolved only after altered protocol was applied.

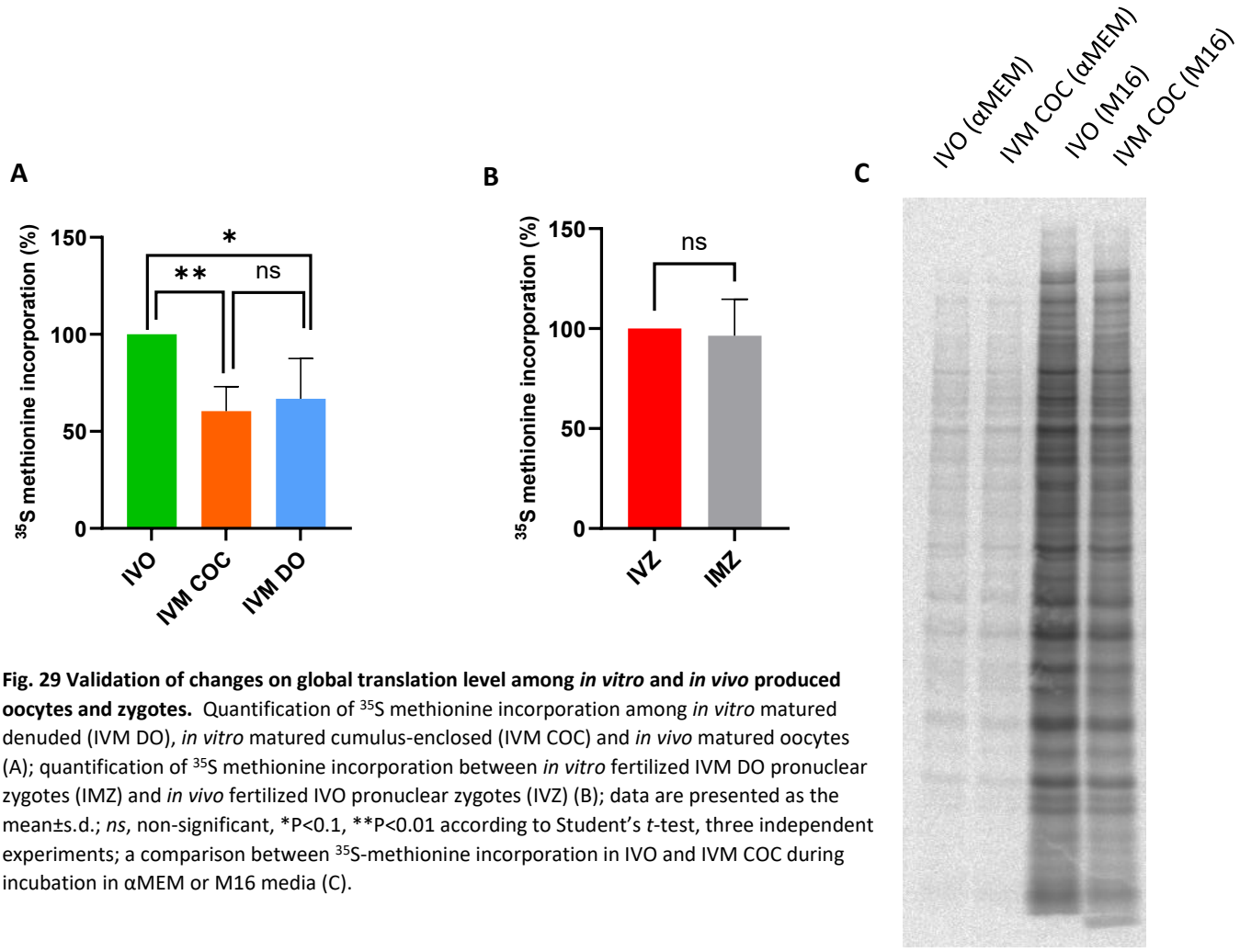

Fig. 29 Validation of changes on global translation level among *in vitro* and *in vivo* produced oocytes and zygotes. Quantification of ^{35}S methionine incorporation among *in vitro* matured denuded (IVM DO), *in vitro* matured cumulus-enclosed (IVM COC) and *in vivo* matured oocytes (A); quantification of ^{35}S methionine incorporation between *in vitro* fertilized IVM DO pronuclear zygotes (IMZ) and *in vivo* fertilized IVO pronuclear zygotes (IVZ) (B); data are presented as the mean±s.d.; *ns*, non-significant, *P<0.1, **P<0.01 according to Student's *t*-test, three independent experiments; a comparison between ^{35}S-methionine incorporation in IVO and IVM COC during incubation in αMEM or M16 media (C).

Strongly suggested fluctuations in energy production between *in vitro* and *in vivo* oocyte maturation as suggested by RNA-seq data (Fig. 30) within MII oocytes were further explored by the Mitotracker staining and subsequent confocal imaging. Much greater mitochondrial clustering in IVO than in IVM COC oocytes was observed (Fig. 31).

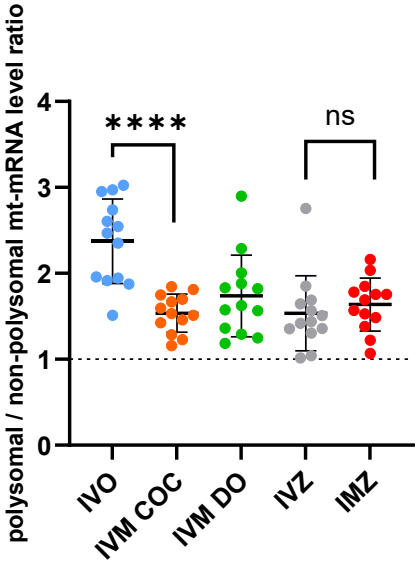

Fig. 30 *In vitro* matured oocytes have lower polysomal/non-polysomal ratio of mitochondrially encoded transcripts. The ratio of normalized polysomal/non-polysomal RNA-seq data (RPKM) of studied *in vitro* and *in vivo* maturation conditions; ****P<0.0001 and ns, non-significant, respectively, according to Student's *t*-test; from four independent experiments.

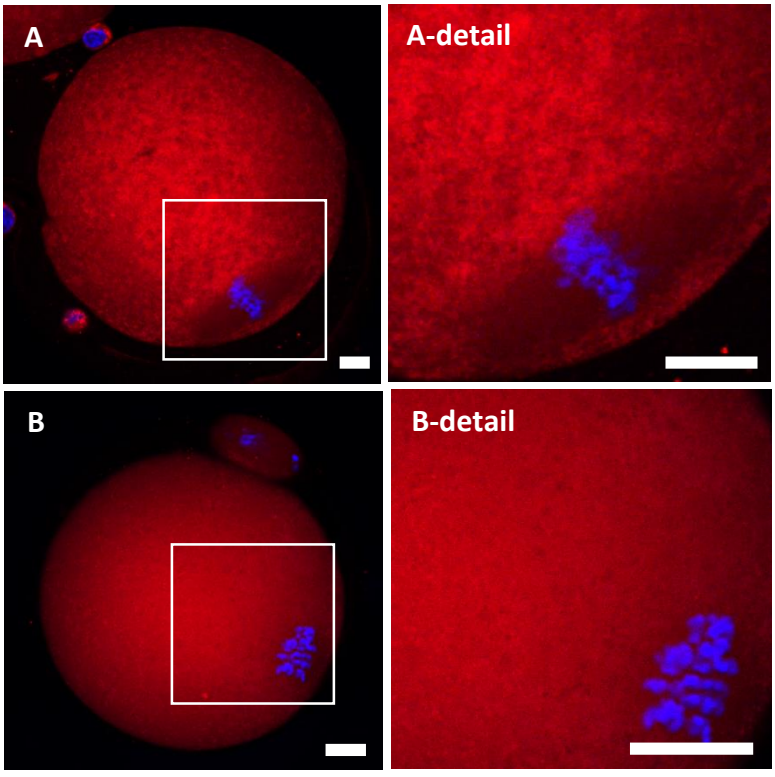

Fig. 31 *In vitro* matured cumulus-oocyte complexes have increased mitochondrial clustering. Mitotracker Red labelled in vivo matured oocyte (IVO) accompanied by progressive clustering within oocyte's cytoplasm (A); Mitotracker Red labelled in vitro matured cumulus-oocyte complex (IVM-COC) accompanied by a smooth pattern of oocyte's cytoplasm (B). Enlarged details are placed on the right. Scale bar 20 µm. Data from three independent experiments, $n \geq 42$

4.8 Assessment of oocyte developmental competence

Hereinabove mentioned IVF technique, was also utilized to assess the complexity of the *in vitro* maturation technology by evaluating early embryo development. It is important to mention, that every IVO, IVM COC and IVM DO replicate was always fertilized with capacitated sperm from the same male. Significant differences in fertilization rate were observed, declining from IVO through IVM COC and towards IVM DO, which yielded about 50 % pronuclear zygotes (Fig. 32).

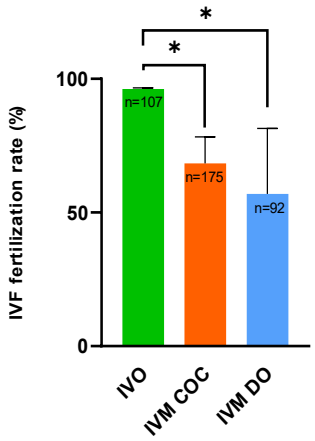

Fig. 32 Ferilization rate significantly decreased in *in vitro* matured oocytes compared to *in vivo* matured. The ratio of normal pronuclear zygotes formed after *in vitro* fertilization of *in vitro* matured denuded oocytes (IVM DO), *in vitro* matured cumulus-oocyte complexes (IVM COC) and *in vivo* matured oocytes (IVO COC). Data are presented as the mean±s.d.; *P<0.1, according to Student's *t*-test; from three independent experiments, *n*≥90.

Subsequent early embryo development yielded about 75-80% blastocysts in IVO COC. Progressive decline of further developing embryos in IVM COC and IVM DO was more or less equal until the 4-cell stage embryo. Beyond this point, IVM DO originated embryos deteriorated faster with significantly lower amount of developed blastocysts than blastocysts originated from IVM COC (Fig. 33, 34).

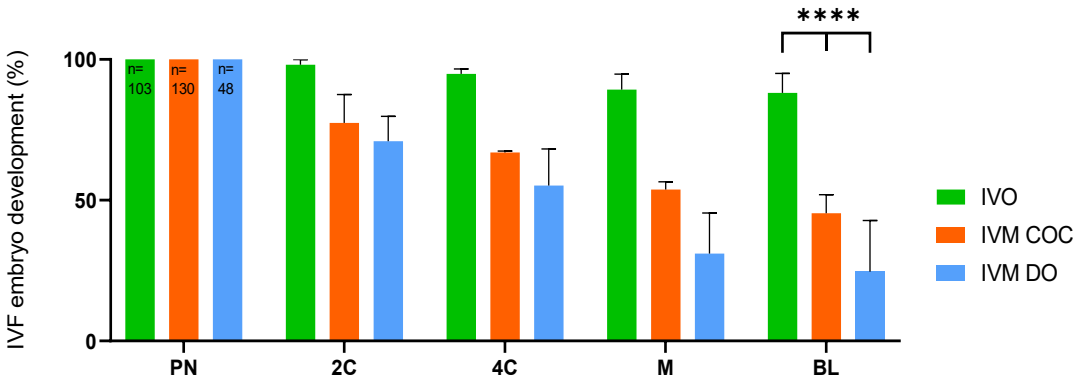

Fig. 33 Embryos raised from *in vitro* matured oocytes gradually deteriorated with the greatest decline in *in vitro* matured denuded oocytes. The ratio of normal 2-cell (2C), 4-cell (4C), morulas(M), or blastocysts (BL) formed after *in vitro* fertilization of *in vitro* matured denuded oocytes (IVM DO), *in vitro* matured cumulus-oocyte complexes (IVM COC) and *in vivo* matured oocytes (IVO COC). Ratio is calculated respectively to the number of pronuclear zygotes. Data are presented as the mean±s.d.; ****P<0.001 according to Two-way ANOVA test; from three independent experiments, *n*≥48

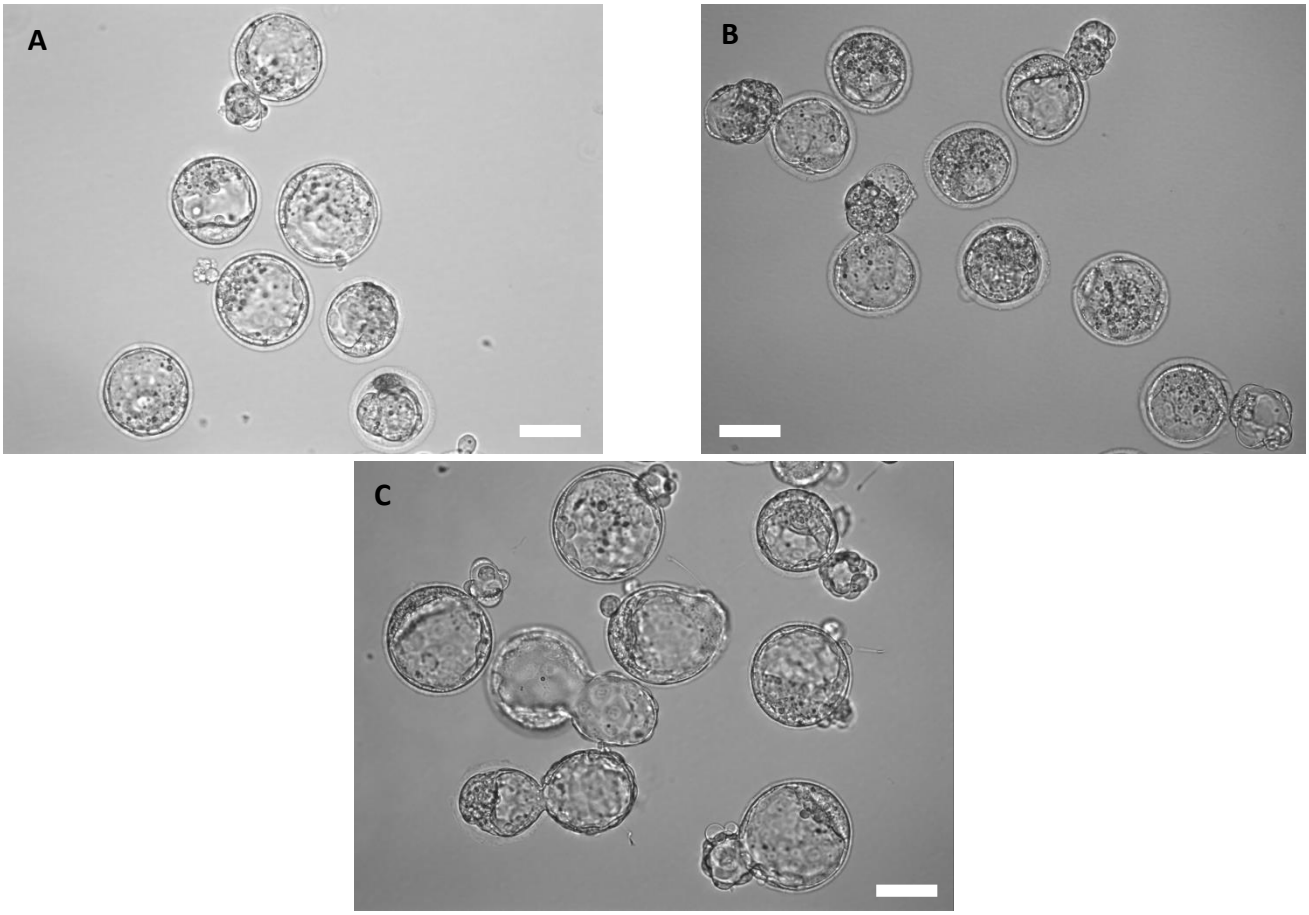

Fig. 34 Blastocysts morphology of in vitro fertilized embryos derived from *in vitro* or *in vivo* matured MII oocytes. Bright-field images of *in vitro* matured denuded oocytes (IVM DO)(A); *in vitro* matured cumulus-oocyte complexes (IVM COC)(B); and *in vivo* matured oocytes (IVO COC)(C); scale bar = 100 µm

5. Discussion

This thesis named: „Characterization of translational patterns in mammalian oocytes and early embryos obtained under different conditions“, is investigating translational pattern at the most profound translation-dependent period of oocyte and embryo development, i.e. the point of fertilizable egg formation as well as upon fertilized pronuclear zygote, still dependent on effective translational regulation of stored maternal transcripts. Both time periods were assessed under different, assisted reproduction (AR) related conditions *in vitro* and *in vivo*.

Being able to reflect in the experimental setting the conventional assisted reproduction technology (ART) was troublesome in many aspects. The initial obstacle was to select the appropriate study model, which was easy to reproduce and synchronize with *in vivo* conditions. Ethically acceptable source of mammalian oocytes were either cows, pigs or mice. Bovine and porcine models although more related to humans than mice with respect to their physiology, had a major disadvantage, which was the inability to precisely set reproducible ovarian stimulation *in vivo* protocol, that was inherently coupled with the ability to optimize and assess *in vivo* meiotic maturation (IVO). The mouse model was comparatively much easier to breed, responded well to superovulation by the pregnant-mare serum gonadotropin (PMSG) and ovulation by recombinant human chorionic gonadotropin (rhCG) with reproducible outcomes. Therefore, it was decided to utilize for experiments the mouse model.

Experimental *in vitro* culture conditions in oocytes and early embryos were set to reflect *in vivo* maturation of the chosen mouse model. Importantly, IVM related molecular processes in ART are not yet clear. As translation and its proper regulation is governing the meiotic part of oocyte maturation and early embryonic development, novel findings in ART-relevant *in vitro* culture conditions could significantly contribute to the field. It was decided to select IVM culture media composition to resemble a clinical one (Wang, Ock and Chian, 2006). Initially selected M16 media did not resemble the basic ART media. Therefore, it was decided to select for experimentation αMEM media, which was supplemented with amino acids, vitamins and bovine serum albumin (BSA). In such media the *in vitro* matured denuded MII oocytes (IVM DO) were cultivated (Fig.7). This composition resembled the rescue-IVM technique, when excessive denuded GV oocytes are *in vitro* matured until the MII stage. Further supplementation of selected αMEM media by a recombinant follicle –stimulating hormone (rFSH) and rhCG was used for IVM of *in vitro* matured cumulus-oocyte complexes (IVM COC) (Fig.7). This setting is most adequately reflecting the conventional IVM in ART (Wang, Ock and Chian, 2006). However, up to the present days, a couple of novel IVM culture strategies, namely stimulated physiological oocyte *in vitro* maturation (SPOM) and biphasic or capacitation *in vitro* maturation (CAPA-IVM) have been developed, which mainly focus on prolonging the initial period from the ovum pick-up (OPU) until the nuclear envelope breakdown (NEBD) (Albuz *et al.*, 2010; Sanchez *et al.*, 2019). These

The collected samples were eventually destined for RNA-seq analysis and therefore it was of utmost importance to synchronize the *in vitro* and *in vivo* maturation and correctly set the exact collection timing to avoid the production of artificial results. The IVM of IVM DO was easy to record, however, the timing to completion of the nuclear maturation, i.e. proper formation of MII spindle, was not possible to define by simple morphological analysis. By applying the IVM DO Live Cell Imaging and labelling the oocytes by sir-tubulin, time needed to form matured MII spindle was extended to approximately 1.5 hours post 1st polar body extrusion (PBE) (Fig. 9). The same phenotype was discovered in ART. In turn, it was suggested to postpone the intra cytoplasmic sperm injection (ICSI) until the nuclear maturation is completed (Holubcová *et al.*, 2019).

The overall IVM timing between the isobutyl-methyl xanthine (IBMX) release and the 1st PBE was almost equal between IVM DO and IVM COC. But, in IVM COC, longer time to NEBD was observed than in the case of IVM DO. However, it was compensated by shorter time from NEBD to 1st PBE (Fig. 17). The delay of IVM COC NEBD may be caused by temporal increase in cyclic adenosine monophosphate (cAMP) due to rFSH and rhCG supplementation (Buccione *et al.*, 1990), preventing activation of maturation promoting factor (MPF). Standard IVM COC in ART is based on supplementation by only rFSH and rLH or its analogue rhCG, in addition to amino acids, vitamins and human serum albumin. Unfortunately, no serum supplementation of culture medium is legally allowed. Culture medium is then deprived of, for example, serum derived inter-α-trypsin inhibitor (Chen *et al.*, 1994) , which is key for branching hyaluronan, stabilizing ECM and ensuring proper COC expansion. In turn, ART-like cultured IVM COC produce less compact COCs (Fig. 18).

The initial plan was to set the time of *in vivo* NEBD by detecting changes in COC expression of amphiregulin (AREG), an epidermal growth factor-like peptide, signalling further on the EGF receptor employed in the meiotic resumption. AREG expression is increased upon LH receptor activation by LH or rhCG (Zamah *et al.*, 2010). Western Blot data showed a shift in IVO COC expression between 3-4 hours post rhCG administration (Fig. 13). However, this experiment only narrowed the expected NEBD window during IVO. Further morphological evaluation of IVO confirmed that around 80-90% had undergone NEBD at 3 hours post rhCG administration *in vivo* (Fig. 14) and within 8 hours around 80-90% of IVO oocytes completed nuclear maturation (Fig. 12). Comparatively, the completion of nuclear maturation *in vitro* from NEBD to 1st PBE took about 9-10 hours, which is about 1-2 hours delay. *In vitro* handling, sub-optimal culture conditions or compromised energy production (Fig. 30) may play a role in delaying IVM in relation to IVO. It was previously reported that inadequate culture supplementation and resulted deficient energy production led to delayed meiotic maturation (Sutton-McDowall, Gilchrist and Thompson, 2010).

IVO collection was initially considered at the point, when IVO COCs were present in infundibulum. Upon further consideration to reflect clinical aspects in the experimental design, IVO collection was set to 11 hours post rhCG administration (Fig. 10), the time point shortly before ovulation, as the OPU in ART is routinely performed before ovulation to avoid losing ovulated MII oocytes within peritoneal cavity. Upon collection nuclearly matured IVO MII spindle was stable for about 5 hours until around 16 hours post hCG,

when the progressive spindle deterioration was observed (Fig. 12). This, relatively rapid, IVO MII spindle destabilisation was accompanied by the movement of chromosomes towards the opposite spindle poles (Fig. 11C-D). This phenotype could be a by-product of the fast *in vivo* post-ovulatory aging within oviducts. Also the absence of capacitated sperm may had caused the failure to receive a feedback signal by the ovulated IVO COC from oviductal isthmic region (Franchi *et al.*, 2020).

Nuclear maturation and MII spindle stability introduced further questions regarding cytoplasmic maturation, which is tightly associated with the state of translatome and stored maternal transcriptome. The data from RNA-seq of SSP-fractionated and total transcriptome were planned to assess changes in translatome and transcriptome. However, firstly, the extent of potential somatic contribution by cumulus cells to IVO was assessed, as previous studies in cows suggested ongoing bidirectional mRNA transport via transzonal projections (TZP) (Macaulay *et al.*, 2014). The results from gap junctional assay suggested the withdrawal of TZPs between 5 – 10 hours post rhCG administration *in vivo* (Fig. 15), which corresponds to 2 – 8 hours post NEBD according to the morphological analysis (Fig. 14). Progressive accumulation of non-permeable and fluorescent Calcein within oocyte cytoplasm, produced by esterase cleavage of permeant Calcein-AM, suggested closure of TZP around half-way through the completion of meiotic maturation. This finding is consistent with the previously reported timing of TZP retraction mechanism dependent on EGF signalling (Abbassi *et al.*, 2021). These data are important regarding the improvement of IVM as ART. If the quality of IVM in AR is to be improved, one of the ways is to better utilize adjacent somatic granulosa cells if available. To do that, TZPs must remain open and granulosa cells nurtured more effectively by improved culture conditions. As it was demonstrated, that under best conditions TZPs close well before ovulation, so improvements must be done prior to NEBD, where oocytes can be held, particularly *in vitro*, for extensive period of time. The CAPA-IVM protocol utilized this rationale to employ physiological signalling pathways in COCs to maintain elevated cGMP and cAMP levels (Sanchez *et al.*, 2019). Clinical data comparing CAPA-IVM with standard IVO & *in vitro* fertilization (IVF) in ART resulted in improved live birth rates (Vuong *et al.*, 2020).

To be able to evaluate developmental competence among oocytes cultures under different conditions, the IVF technology was needed. As this technique was not performed in our laboratory before, the initial guidelines were adopted from a recent publication (Takeo, Sztein and Nakagata, 2019). First few IVF experiments in the mouse model did not produce fertilized zygotes, however after improving sperm capacitation by supplementing capacitation media with reduced-glutathione and bovine serum albumin, fertilization and embryo development was achieved. The IVF protocol was very sensitive for the quality of used paraffin oil, fine removal of adipose tissue or proper sperm extraction from cauda epididymis under oil. Acquisition of 80% blastocysts rate from IVO COCs (Fig. 19) validated the IVF protocol for further applications. One of the first IVF experimental outcomes was the benefit of foetal bovine serum (FBS) over bovine serum albumin (BSA) in IVM COC. Set ART-like IVM COC media supplemented with either FBS or BSA showed different morphological characteristics (Fig. 18) with the former one resembling more IVO collected COCs. IVF data uncovered much better developmental competence of FBS supplemented IVM COC (Fig. 19).

However, FBS, human serum or even allogenic maternal serum is not legally allowed to be included in ART at the present time. Maternal serum supplementation experiments were published in humans more than 20 years ago (Mikkelsen *et al.*, 2001) and the approach is still not adopted in ART.

Setting up the process of *in vivo* fertilization in mice was quite difficult as it had to be approximated from individual observations. It was confirmed that ovulation *in vivo* is happening about 12 hours post hCG administration (Fig. 10). The pronuclear NEBD was set as the reference point in *in vivo* pronuclear zygotes (IVZ) to retrospectively estimate *in vivo* fertilization time. As male mating was done overnight, it could be assumed the sperm was capacitated within isthmic region and waiting for the signal from oviduct – COC interaction (Franchi *et al.*, 2020) that happened no earlier than 12-13 hours post rhCG administration, because of meiotic maturation and ovulation. The in vitro fertilized IVM DO pronuclear zygotes (IMZ) were collected 8 hours post IVF. As the time between fertilization and pronuclear NEBD was not significantly different (Fig. 21) between IVZ and IMZ, IVZ collection corresponded to 7-8 hours post *in vivo* fertilization, i.e. at 20 hours post rhCG administration. Previously published IVF experiments monitoring transcription using labelled bromouridine, revealed that 12 hours post IVF, a minor zygotic genome transcription is activated (ZGA) (Abe *et al.*, 2018). This clearly implies that analysed zygotic transcriptomes and translatomes were of maternal origin.

The differential gene expression (DGE) analysis of polysome-derived RNA-seq data revealed significant changes in translation between *in vitro* and *in vivo* matured oocytes and subsequent the fertilization in zygotes, but surprisingly, the global changes were more subtle than was expected. Selected ART-like IVM culture media supplemented with amino acids and a variation of vitamins to support developmental competence, could have potentially suppressed the negative effect of reactive oxygen species by for example IVM media-included vitamin C (Qin *et al.*, 2022; Rakha *et al.*, 2022).

In vitro vs. *in vivo* studies conducted on clinical samples in the past compared only changes in total transcriptomes or proteomes. A microarray gene expression study on human oocytes (Wells and Patrizio, 2008) observed extensive overlap among IVM and IVO groups, which is in good agreement with our data. On the contrary, the same year, another microarray study reported more than 2 000 upregulated transcripts in human IVM compared to IVO (Jones *et al.*, 2008). Particularly, the gene ontology (GO) terms showed correlation with our data, i.e. cell cycle, DNA damage repair, or RNA metabolism. Almost a decade later with advent of single-cell RNA-seq technology (Borensztein *et al.*, 2018), a study on mouse IVM oocytes reported significant alterations to mitochondrial metabolism (Gao *et al.*, 2017). This finding was not only supporting our data, but also GO data of previous microarray based publications (Jones *et al.*, 2008; Wells and Patrizio, 2008). Changes to mitochondrial-related transcripts were also detected in recent sc-RNA-seq comparison between rescue-IVM and IVO in humans. However, the ambiguity of acquired findings may had been introduced by oocyte maturation under hypoxic conditions (Lee *et al.*, 2021). A group by (Guo *et al.*, 2022) claimed high proteome heterogeneity between *in vitro* and *in vivo* oocytes, however, the IVM culture protocol corresponded to rescue-IVM with post-ovulatory collected GV oocytes of inferior quality.

The gene ontology enrichment analysis (GOEA) of differentially expressed (DE) IVM DO - IVM COC pointed out changes in protein synthesis. Detected decrease of protein synthesis related transcripts of IVM DO *vs.* IVM COC was in concordance with decreased, however, not significant, incorporation level of radioactive ^{35}S-methionine labelling, which was indicative of changes in global translation. Generally, the decreased protein synthesis in IVM COC in comparison with IVO or IVM DO could be attributed to either presence of cumulus cells or rFSH and rhCG administration. Based on the comparison of IVM COC and IVO significance, decreased protein synthesis is more likely to be linked to gonadotropin administration. Previous findings confirmed the rFSH effect on decreased global translation across various mammalian species including humans (Tetkova *et al.*, 2019).

Minor but significant increase of AURKA expression Fig. 27A) may be attributed to destabilized IVM oocyte spindle integrity, because it is a serine/threonine kinase required for proper spindle pole focusing, formation of liquid-like spindle domain and for the regulation of Transforming Acidic Coiled-Coil Containing Protein 3 (TACC3) (Blengini et al., 2021). A recent publication on mouse oocytes found TACC3 presence to be essential for nucleation of human microtubule organizing centres (Wu et al., 2022). The second studied protein, Centromere Protein V (CENPV), was recently shown to be important for proper chromosome segregation as it is involved in microtubule-kinetochore attachment and its deficiency can lead to weakening the spindle assembly checkpoint (Nabi *et al.*, 2021). Western Blot data demonstrated the significantly decreased level of CENPV in IVM DO, which is about 75% of IVO (Fig. 27B). The functional role of this decrease is, however, still questionable, it may contribute to multifactorial decrease of spindle stability in MII and become a basis for aneuploidy. The similar pattern was observed in Sperm Associated Antigen 5 (SPAG5) or also called Astrin. This protein, however not validated here, was differentially expressed between *in vitro* and *in vivo* matured oocytes. SPAG5 is reported to be involved in spindle pole integrity and may interact with AURKA and PLK1 (Yuan *et al.*, 2009). Deficient SPAG5 in IVM DO may be associated with well-known phenomenon of barrel-shaped spindles in IVM oocytes (Sanfins *et al.*, 2003).

The transcripts displaying significantly different association with polysomes in both IVM DO and IVM COC were also related to energy production. Indeed, mtRNA transcripts, encoding proteins employed in energy production, were more translated in IVO than in IVM COC or IVM DO (Fig. 30). Moreover, increased mitochondrial clustering in IVO compared to IVM COC, which was analysed by confocal microscopy (Fig. 31), was indicative of increased ATP production as previously published in mouse oocytes (Yu *et al.*, 2010).

Poly(A) specific ribonuclease (PARN) and NOP2/Sun RNA methyltransferase 2 (NSUN2) proteins were selected for Western Blot validation as they represent DE transcripts in the comparison of pronuclear zygotes and are also enriched in GO term “RNA metabolism”. PARN protein activity has a clear impact on the zygote function as it was recently found to play a role in embryogenesis, cell-cycle regulation, telomere function, etc. (Nanjappa *et al.*, 2021). Our validation experiments by Western Blot showed decreased protein level in IMZ to about 60% of IVZ (Fig. 28), which also correlated with the RNA-seq data. The next RNA-seq

candidate, NSUN2, has recently been shown to stabilize mRNAs via epigenetic m^5C modification in *Plasmodium* (Liu *et al.*, 2022). The difference between IMZ and IVZ was confirmed by Western Blot results. A significant decrease of NSUN2 protein level by 25% in IMZ relative to IVZ was observed (Fig. 28). It could by hypothesized that NSUN2 may be crucial for epigenetic stabilization of particular mRNA transcripts as MII oocytes progress through the maternal - zygotic transition. Detected NSUN2 deficiency in IMZ may be a reason why some key mRNA transcripts are degraded.

To appreciate a broader view on the complexity of the IVM and IVO system, particularly with relevance to ART, the developmental competence in IVM DO, IVM COC and IVO was assessed by the IVF. Fertilization rate in IVM DO, corresponding to rescue-IVM, halved with respect to IVO conditions. IVM COCs that reflected conventional IVM culture conditions in ART provided a minor improvement to fertilization rate (Fig. 31). Further decrease in developmental competence of embryos derived from *in vitro* matured oocytes was expected. However, it was surprising to notice progressive diversion between the amount of viable embryos between IVM DO and IVM COC beyond the 4-cell stage (Fig. 32). Differential gene expression (DGE) analysis detected only few DE polysomal transcripts (Fig. 25) as well as there was no significant difference observed on the global protein synthesis detected by ^{35}S-methionine labelling (Fig. 29). These facts together suggest that difference in developmental potential between IVM DO - IVM COC culture is connected with embryonic genome activation in mice that occurs around the 2-cell stage. However whether some dormant transcripts are passed through TZPs within the first half of meiotic maturation or cumulus cells create a protective layer or buffer changes within surrounding environment remain unclear. It is worth to stress again that further serum supplementation has overcome developmental potential of ART-relevant IVM COC. The recue-IVM is somehow similar to IVM DO and its very low fertilization rates are known and therefore it is selected only as the option of last-resort, when no or a very few matured *in vivo* MII oocytes are collected by OPU (Lee *et al.*, 2016).

Characterization of translational patterns in mouse MII oocytes and derived pronuclear zygotes developed under *in vitro* or *in vivo* maturation conditions surprisingly resulted in higher similarity than initially expected. Data from RNA-seq analysis of SSP-fractionated samples unravelled greatest differences in terms of active translation between ART-relevant IVM COC and IVO, related to the cell cycle regulation, energy production or protein synthesis. However, IVM COC had higher developmental competency in terms of blastocyst rate than IVM DO originated embryos. This may be associated with defects in embryonic genome activation as the developmental progress of IVM DO originated embryos deteriorated from the 4-cell embryo onwards (Fig. 33). Indirectly our RNA-seq results as well as gap-junctional assay results (Fig. 15) support the ART-related novel strategies like for example CAPA-IVM, which support the prolonged somatic cells-oocyte communication via TZPs at the point of arrested fully grown GV oocyte prior to their closure following NEBD.

6. Conclusions

- The term various culture conditions was successfully employed to compare translational patterns between *in vitro* and *in vivo* conditions in mammalian MII oocytes and pronuclear zygotes using the mouse model

- IVM COC culture (conventional) as well IVM DO (rescue) culture was set to reflect relevant assisted reproduction techniques

- The progress of *in vivo* maturation was mapped in the mouse model and IVM DO & IVM COC were adjusted to be synchronized and produced valuable data

- *In vitro* fertilization protocol was optimized in our laboratory. As a results, IMZ samples were collected and credible developmental competence data were produced

- Polysome profiling was successfully performed in all studies culture conditions according to the Scarce Sample Profiling protocol.

- cDNA libraries and NGS RNA-seq data were successfully obtained for polysomal, non-polysomal RNA fractions and total RNA.

- Differential gene expression analysis coupled with Gene ontology enrichment analysis uncovered significant differences in actively translated transcripts between IVM COC and IVO with selected transcripts employed in cell cycle regulation, DNA repair, protein synthesis, and energy production.

- Differential gene expression analysis between IMZ and IVZ pronuclear zygotes showed also changes on polysomal level related to RNA metabolism, cell cycle regulation or spindle assembly checkpoint.

- Developmental competence assessment of IVM DO, IVM COC and IVO by IVF confirmed superior developmental competence of IVM COC over IVM DO, in particular on blastocyst rates. Addition of foetal bovine serum to IVM COC significantly increased blastocyst rates towards IVO.

7. References

Abbassi, L. *et al.* (2021) 'Epidermal growth factor receptor signaling uncouples germ cells from the somatic follicular compartment at ovulation', *Nature Communications*, 12(1), pp. 1–13. doi: 10.1038/s41467-021-21644-z.

Abe, K. ichiro *et al.* (2018) 'Minor zygotic gene activation is essential for mouse preimplantation development', *Proceedings of the National Academy of Sciences of the United States of America*, 115(29), pp. E6780–E6788. doi: 10.1073/pnas.1804309115.

Albuz, F. K. *et al.* (2010) 'Simulated physiological oocyte maturation (SPOM): A novel in vitro maturation system that substantially improves embryo yield and pregnancy outcomes', *Human Reproduction*, 25(12), pp. 2999–3011. doi: 10.1093/humrep/deq246.

Asami, M. *et al.* (2022) 'Human embryonic genome activation initiates at the one-cell stage', *Cell stem cell*, 29(2), pp. 209-216.e4. doi: 10.1016/J.STEM.2021.11.012.

Blengini, C. S. *et al.* (2021) 'Aurora kinase A is essential for meiosis in mouse oocytes', *PLoS genetics*, 17(4). doi: 10.1371/JOURNAL.PGEN.1009327.

Borensztein, M. *et al.* (2018) 'Transcriptome Profiling of Single Mouse Oocytes', *Methods in molecular biology (Clifton, N.J.)*, 1818, pp. 51–65. doi: 10.1007/978-1-4939-8603-3_7.

Bromfield, J. J. and Piersanti, R. L. (2019) 'Mammalian Oogenesis: The Fragile Foundation of the Next Generation', *The Ovary*, pp. 157–164. doi: 10.1016/B978-0-12-813209-8.00010-8.

Buccione, R. *et al.* (1990) 'FSH-induced expansion of the mouse cumulus oophorus in vitro is dependent upon a specific factor(s) secreted by the oocyte', *Developmental biology*, 138(1), pp. 16–25. doi: 10.1016/0012-1606(90)90172-F.

Carlson, L. J. and Shaw, N. D. (2019) 'Development of Ovulatory Menstrual Cycles in Adolescent Girls', *Journal of pediatric and adolescent gynecology*, 32(3), pp. 249–253. doi: 10.1016/J.JPAG.2019.02.119.

Chen, L. *et al.* (1994) 'Tm JOURNAL OF BIOLOGICAL CHEMISTRY Proteins of the Inter-a-trypsin Inhibitor Family Stabilize the Cumulus Extracellular Matrix through Their Direct Binding with Hyaluronic Acid*', 269(45), pp. 28282–28287. doi: 10.1016/S0021-9258(18)46925-6.

Cheng, S. *et al.* (2022) 'Mammalian oocytes store mRNAs in a mitochondria-associated membraneless compartment.', *Science (New York, N.Y.)*, 378(6617), p. eabq4835. doi: 10.1126/science.abq4835.

Chian, R. C. *et al.* (2023) 'IVM of human immature oocytes for infertility treatment and fertility preservation', *Reproductive Medicine and Biology*, 22(1), p. e12524. doi: 10.1002/RMB2.12524.

Dai, X. X. *et al.* (2019) 'A combinatorial code for mRNA 3'-UTR-mediated translational control in the mouse oocyte', *Nucleic Acids Research*, 47(1), pp. 328–340. doi: 10.1093/nar/gky971.

Despic, V. and Neugebauer, K. M. (2018) 'RNA tales - how embryos read and discard messages from mom', *Journal of Cell Science*, 131(5). doi: 10.1242/jcs.201996.

Dolmans, M.-M. *et al.* (2021) 'Fertility Preservation: How to Preserve Ovarian Function in Children, Adolescents and Adults.', *Journal of clinical medicine*, 10(22). doi: 10.3390/jcm10225247.

Dvoran, M., Nemcova, L. and Kalous, J. (2022) 'An Interplay between Epigenetics and Translation in Oocyte Maturation and Embryo Development: Assisted Reproduction Perspective', *Biomedicines*, 10(7). doi: 10.3390/BIOMEDICINES10071689.

ESHRE (2016) 'The maturity of in vitro maturation', (January).

Fan, H.-Y. and Sun, Q.-Y. (2019) 'Oocyte Meiotic Maturation', *The Ovary*, pp. 181–203. doi: 10.1016/B978-0-

12-813209-8.00012-1.

Fancsovits, P. *et al.* (2022) 'Prospective-randomized study comparing clinical outcomes of IVF treatments where embryos were cultured individually or in a microwell group culture dish', *Biologia Futura*, 73(2), pp. 229–236. doi: 10.1007/S42977-022-00113-8/TABLES/5.

Franchi, A. *et al.* (2020) 'Extracellular vesicles from oviductal isthmus and ampulla stimulate the induced acrosome reaction and signaling events associated with capacitation in bovine spermatozoa', *Journal of Cellular Biochemistry*, 121(4), pp. 2877–2888. doi: 10.1002/JCB.29522.

Gao, L. *et al.* (2017) 'RNA-Seq transcriptome profiling of mouse oocytes after in vitro maturation and/or vitrification', *Scientific Reports*, 7(1), pp. 1–10. doi: 10.1038/s41598-017-13381-5.

Guo, Y. *et al.* (2022) 'Single-Cell Quantitative Proteomic Analysis of Human Oocyte Maturation Revealed High Heterogeneity in In Vitro–Matured Oocytes', *Molecular & Cellular Proteomics*, 21(8), p. 100267. doi: 10.1016/J.MCPRO.2022.100267.

Harrison, S. E., Sozen, B. and Zernicka-Goetz, M. (2018) 'In vitro generation of mouse polarized embryo-like structures from embryonic and trophoblast stem cells', *Nature Protocols*, 13(7), pp. 1586–1602. doi: 10.1038/s41596-018-0005-x.

Hikabe, O. *et al.* (2016) 'Reconstitution in vitro of the entire cycle of the mouse female germ line', *Nature 2016 539:7628*, 539(7628), pp. 299–303. doi: 10.1038/nature20104.

Holubcová, Z. *et al.* (2019) 'Egg maturity assessment prior to ICSI prevents premature fertilization of late-maturing oocytes', *Journal of Assisted Reproduction and Genetics*, 36(3), pp. 445–452. doi: 10.1007/s10815-018-1393-0.

Houghton, F. D. (2021) 'HYPOXIA AND REPRODUCTIVE HEALTH: Hypoxic regulation of preimplantation embryos: lessons from human embryonic stem cells', *Reproduction*, 161(1), pp. F41–F51. doi: 10.1530/REP-20-0322.

Ingolia, N. T. (2016) 'Ribosome Footprint Profiling of Translation throughout the Genome', *Cell*, 165(1), pp. 22–33. doi: 10.1016/j.cell.2016.02.066.

Jansova, D. *et al.* (2018) 'Localization of RNA and translation in the mammalian oocyte and embryo', *PLoS ONE*, 13(3), pp. 1–25. doi: 10.1371/journal.pone.0192544.

Jones, G. M. *et al.* (2008) 'Gene expression profiling of human oocytes following in vivo or in vitro maturation', *Human reproduction (Oxford, England)*, 23(5), pp. 1138–1144. doi: 10.1093/HUMREP/DEN085.

Lee, A. W. T. *et al.* (2021) 'Single-cell RNA sequencing identifies molecular targets associated with poor in vitro maturation performance of oocytes collected from ovarian stimulation', *Human reproduction (Oxford, England)*, 36(7), pp. 1907–1921. doi: 10.1093/HUMREP/DEAB100.

Lee, H. J. *et al.* (2016) 'Rescue in vitro maturation (IVM) of immature oocytes in stimulated cycles in women with low functional ovarian reserve (LFOR)', *Endocrine*, 52(1), pp. 165–171. doi: 10.1007/S12020-015-0744-1.

Li, J., Mao, G. and Xia, G. (2012) 'FSH Modulates PKAI and GPR3 Activities in Mouse Oocyte of COC in a Gap Junctional Communication (GJC)-Dependent Manner to Initiate Meiotic Resumption', *PLoS ONE*, 7(9). doi: 10.1371/journal.pone.0037835.

Li, Y. *et al.* (2023) 'Extracellular vesicles from human Fallopian tubal fluid benefit embryo development in vitro', *Human Reproduction Open*, 2023(2). doi: 10.1093/HROPEN/HOAD006.

Liu, M. *et al.* (2022) '5-methylcytosine modification by Plasmodium NSUN2 stabilizes mRNA and mediates the development of gametocytes', *Proceedings of the National Academy of Sciences of the United States of America*, 119(9). doi: 10.1073/PNAS.2110713119/-/DCSUPPLEMENTAL.

Macaulay, A. D. *et al.* (2014) 'The gametic synapse: RNA transfer to the bovine oocyte', *Biology of Reproduction*, 91(4), pp. 1–12. doi: 10.1095/BIOLREPROD.114.119867/2434303.

Marcelo, A. *et al.* (2021) 'Stress granules, RNA-binding proteins and polyglutamine diseases: too much aggregation?', *Cell Death & Disease 2021 12:6*, 12(6), pp. 1–17. doi: 10.1038/s41419-021-03873-8.

Masek, T. *et al.* (2020) 'Identifying the Translatome of Mouse NEBD-Stage Oocytes via SSP-Profiling; A Novel Polysome Fractionation Method', *International journal of molecular sciences*, 21(4). doi: 10.3390/IJMS21041254.

Mikkelsen, A. *et al.* (2001) 'Maternal serum supplementation in culture medium benefits maturation of immature human oocytes', *Reproductive BioMedicine Online*, 3(2), pp. 112–116. doi: 10.1016/S1472-6483(10)61978-5.

Moolhuijsen, L. M. E. and Visser, J. A. (2020) 'Anti-Müllerian Hormone and Ovarian Reserve: Update on Assessing Ovarian Function', *The Journal of clinical endocrinology and metabolism*, 105(11). doi: 10.1210/CLINEM/DGAA513.

Nabi, D. *et al.* (2021) 'CENP-V is required for proper chromosome segregation through interaction with spindle microtubules in mouse oocytes', *Nature Communications*, 12(1). doi: 10.1038/s41467-021-26826-3.

Nagyová, E., Němcová, L. and Camaioni, A. (2022) 'Cumulus Extracellular Matrix Is an Important Part of Oocyte Microenvironment in Ovarian Follicles: Its Remodeling and Proteolytic Degradation', *International Journal of Molecular Sciences*, 23(1). doi: 10.3390/IJMS23010054.

Nanjappa, D. P. *et al.* (2021) 'Poly (A)-specific ribonuclease (PARN): More than just "mRNA stock clearing"', *Life sciences*, 285. doi: 10.1016/J.LFS.2021.119953.

Nguyen Thanh, T., Doan Thi, H. and Quan Hoang, L. (2018) 'The Spindle of Oocytes Observed by Polarized Light Microscope Can Predict Embryo Quality', *J Gynecol Women's Health*, 9(4). doi: 10.19080/JGWH.2018.09.555766.

O'Brien, M. J., Pendola, J. K. and Eppig, J. J. (2003) 'A revised protocol for in vitro development of mouse oocytes from primordial follicles dramatically improves their developmental competence', *Biology of Reproduction*, 68(5), pp. 1682–1686. doi: 10.1095/biolreprod.102.013029.

Oldak, B. *et al.* (2023) 'Complete human day 14 post-implantation embryo models from naive ES cells', *Nature 2023 622:7983*, 622(7983), pp. 562–573. doi: 10.1038/s41586-023-06604-5.

Pan, B. and Li, J. (2019) 'The art of oocyte meiotic arrest regulation', *Reproductive Biology and Endocrinology*, 17(1), pp. 1–12. doi: 10.1186/s12958-018-0445-8.

Paulini, F. and Melo, E. O. (2011) 'The role of oocyte-secreted factors GDF9 and BMP15 in follicular development and oogenesis', *Reproduction in domestic animals = Zuchthygiene*, 46(2), pp. 354–361. doi: 10.1111/J.1439-0531.2010.01739.X.

Qin, H. *et al.* (2022) 'In Vivo and In Vitro Matured Oocytes From Mice of Advanced Reproductive Age Exhibit Alternative Splicing Processes for Mitochondrial Oxidative Phosphorylation', *Frontiers in endocrinology*, 13. doi: 10.3389/FENDO.2022.816606.

Rakha, S. I. *et al.* (2022) 'Importance of Antioxidant Supplementation during In Vitro Maturation of Mammalian Oocytes', *Veterinary sciences*, 9(8). doi: 10.3390/VETSCI9080439.

Rehnitz, J. *et al.* (2017) 'FMR1 and AKT/mTOR signalling pathways: potential functional interactions controlling folliculogenesis in human granulosa cells', *Reproductive BioMedicine Online*, 35(5), pp. 485–493. doi: 10.1016/j.rbmo.2017.07.016.

Richani, D. and Gilchrist, R. B. (2018) 'The epidermal growth factor network: Role in oocyte growth, maturation and developmental competence', *Human Reproduction Update*, 24(1), pp. 1–14. doi: 10.1093/humupd/dmx029.

Rodrigues, P. *et al.* (2023) 'In vitro maturation of oocytes as a laboratory approach to polycystic ovarian syndrome (PCOS): From oocyte to embryo', *WIREs mechanisms of disease*. doi: 10.1002/WSBM.1600.

Russell, D. L. and Robker, R. L. (2019) 'Ovulation: The Coordination of Intrafollicular Networks to Ensure Oocyte Release', *The Ovary*, pp. 217–234. doi: 10.1016/B978-0-12-813209-8.00014-5.

Sanchez, F. *et al.* (2019) 'Biphasic in vitro maturation (CAPA-IVM) specifically improves the developmental capacity of oocytes from small antral follicles', *Journal of assisted reproduction and genetics*, 36(10), pp. 2135–2144. doi: 10.1007/S10815-019-01551-5.

Sanfins, A. *et al.* (2003) 'Distinctions in Meiotic Spindle Structure and Assembly during In Vitro and In Vivo Maturation of Mouse Oocytes', *Biology of Reproduction*, 69(6), pp. 2059–2067. doi: 10.1095/biolreprod.103.020537.

Sanfins, A. *et al.* (2004) 'Meiotic spindle morphogenesis in in vivo and in vitro matured mouse oocytes: Insights into the relationship between nuclear and cytoplasmic quality', *Human Reproduction*, 19(12), pp. 2889–2899. doi: 10.1093/humrep/deh528.

Sanz, E. *et al.* (2019) 'RiboTag: Ribosomal Tagging Strategy to Analyze Cell Type Specific mRNA Expression In Vivo', *Current protocols in neuroscience*, 88(1), p. e77. doi: 10.1002/CPNS.77.

Shuhaibar, L. C. *et al.* (2015) 'Intercellular signaling via cyclic GMP diffusion through gap junctions restarts meiosis in mouse ovarian follicles', *Proceedings of the National Academy of Sciences of the United States of America*, 112(17), pp. 5527–5532. doi: 10.1073/pnas.1423598112.

Standart, N. and Weil, D. (2018) 'P-Bodies: Cytosolic Droplets for Coordinated mRNA Storage', *Trends in Genetics*, 34(8), pp. 612–626. doi: 10.1016/J.TIG.2018.05.005.

Su, Y. Q. *et al.* (2007) 'Selective degradation of transcripts during meiotic maturation of mouse oocytes', *Developmental Biology*, 302(1), pp. 104–117. doi: 10.1016/j.ydbio.2006.09.008.

Sun, X. *et al.* (2023) 'Comprehensive analysis of nonsurrounded nucleolus and surrounded nucleolus oocytes on chromatin accessibility using ATAC-seq', *Molecular reproduction and development*, 90(2), pp. 87–97. doi: 10.1002/MRD.23668.

Susor, A. *et al.* (2015) 'Temporal and spatial regulation of translation in the mammalian oocyte via the mTOR-eIF4F pathway', *Nature Communications*, 6, pp. 1–12. doi: 10.1038/ncomms7078.

Šušor, A. *et al.* (2008) 'Regulation of cap-dependent translation initiation in the early stage porcine parthenotes', *Molecular reproduction and development*, 75(12), pp. 1716–1725. doi: 10.1002/MRD.20913.

Susor, A. and Kubelka, M. (2017) *Translational regulation in the mammalian oocyte*, *Results and Problems in Cell Differentiation*. doi: 10.1007/978-3-319-60855-6_12.

Sutton-McDowall, M. L., Gilchrist, R. B. and Thompson, J. G. (2010) 'The pivotal role of glucose metabolism in determining oocyte developmental competence', *Reproduction*, 139(4), pp. 685–695. doi: 10.1530/REP-09-0345.

Takeo, T., Sztein, J. and Nakagata, N. (2019) 'The CARD Method for Mouse Sperm Cryopreservation and In Vitro Fertilization Using Frozen-Thawed Sperm', *Methods in molecular biology (Clifton, N.J.)*, 1874, pp. 243–256. doi: 10.1007/978-1-4939-8831-0_14.

Teede, H. J. *et al.* (2023) 'Recommendations from the 2023 International Evidence-based Guideline for the Assessment and Management of Polycystic Ovary Syndrome', *Human Reproduction*, 38(9), pp. 1655–1679. doi: 10.1093/HUMREP/DEAD156.

Tetkova, A. *et al.* (2019) 'Follicle-stimulating hormone administration affects amino acid metabolism in mammalian oocytes†', *Biology of reproduction*, 101(4), pp. 719–732. doi: 10.1093/BIOLRE/IOZ117.

Thoreen, C. C. *et al.* (2012) 'A unifying model for mTORC1-mediated regulation of mRNA translation', *Nature*, 485(7396), pp. 109–113. doi: 10.1038/nature11083.

Trebichalská, Z. *et al.* (2021) 'Cytoplasmic maturation in human oocytes: An ultrastructural study', *Biology of Reproduction*, 104(1), pp. 106–116. doi: 10.1093/biolre/ioaa174.

Vuong, L. N. *et al.* (2020) 'In-vitro maturation of oocytes versus conventional IVF in women with infertility and a high antral follicle count: A randomized non-inferiority controlled trial', *Human Reproduction*, 35(11), pp. 2537–2547. doi: 10.1093/humrep/deaa240.

Wang, Y., Ock, S. A. and Chian, R. C. (2006) 'Effect of gonadotrophin stimulation on mouse oocyte quality and subsequent embryonic development in vitro', *Reproductive BioMedicine Online*, 12(3), pp. 304–314. doi: 10.1016/S1472-6483(10)61002-4.

Wang, Z. *et al.* (2022) 'The oocyte cumulus complex regulates mouse sperm migration in the oviduct', *Communications Biology 2022 5:1*, 5(1), pp. 1–12. doi: 10.1038/s42003-022-04287-8.

Wells, D. and Patrizio, P. (2008) 'Gene expression profiling of human oocytes at different maturational stages and after in vitro maturation', *American journal of obstetrics and gynecology*, 198(4), pp. 455.e1-455.e11. doi: 10.1016/J.AJOG.2007.12.030.

Wu, T. *et al.* (2022) 'The mechanism of acentrosomal spindle assembly in human oocytes', *Science (New York, N.Y.)*, 378(6621). doi: 10.1126/SCIENCE.ABQ7361.

Xie, Y. *et al.* (2018) 'Oocyte-specific deletion of Gsα induces oxidative stress and deteriorates oocyte quality in mice', *Experimental Cell Research*, 370(2), pp. 579–590. doi: 10.1016/j.yexcr.2018.07.023.

Yan, L. *et al.* (2013) 'Single-cell RNA-Seq profiling of human preimplantation embryos and embryonic stem cells', *Nature Structural & Molecular Biology 2013 20:9*, 20(9), pp. 1131–1139. doi: 10.1038/nsmb.2660.

Yang, H. *et al.* (2021) 'Factors Influencing the In Vitro Maturation (IVM) of Human Oocyte', *Biomedicines*, 9(12). doi: 10.3390/BIOMEDICINES9121904.

Yu, Y. *et al.* (2010) 'Redistribution of mitochondria leads to bursts of ATP production during spontaneous mouse oocyte maturation', *Journal of Cellular Physiology*, 224(3), pp. 672–680. doi: 10.1002/jcp.22171.

Yuan, J. *et al.* (2009) 'Astrin regulates meiotic spindle organization, spindle pole tethering and cell cycle progression in mouse oocytes', *Cell Cycle*, 8(20), pp. 3384–3395. doi: 10.4161/cc.8.20.9885.

Zamah, A. M. *et al.* (2010) 'Human oocyte maturation is dependent on LH-stimulated accumulation of the epidermal growth factor-like growth factor, amphiregulin', *Human reproduction (Oxford, England)*, 25(10), pp. 2569–2578. doi: 10.1093/HUMREP/DEQ212.

Zhu, L. *et al.* (2022) 'High-resolution ribosome profiling reveals translational selectivity for transcripts in bovine preimplantation embryo development', *Development (Cambridge, England)*, 149(21). doi: 10.1242/DEV.200819.

Zhu, Y. *et al.* (2022) 'Mettl3 downregulation in germinal vesicle oocytes inhibits mRNA decay and the 1st polar body extrusion during maturation', *Biology of reproduction*. doi: 10.1093/BIOLRE/IOAC112.

8. Comments on associated publications

Lamacova L., Jansova D., Jiang Z., **Dvoran M.**, Aleshkina D., Iyyappan R., Jindrova A., Fan H.Y., Gao Y., Susor A. 'Absence of CPEB3 in the egg leads to early embryo lethality', under review

- *Research article with contribution in experimental part, where I took part in polysome fractionation, radioactive methionine labelling and proofreading of the revised article.*

Iyyappan R., Aleshkina D., Ming H., **Dvoran M.**, Kakavand K., Jansova D., del Llano, E., Gahurova L., Bruce A.W., Masek T., Pospisek M., Horvat F., Kubelka M., Jiang Z., Susor A. (2023) 'The translational oscillation in oocyte and early embryo development', Nucleic Acids Research, 1-16. doi: 10.1093/nar/gkad996

- *Research article with contribution in both experimental and review part. I took part in polysome fractionation, in vitro fertilization experiments, data analysis as well as in revision part where I performed experiments on an additional eEF2 inhibitor and co-created complementary graphical abstract.*

Dvoran, M., Nemcova, L. and Kalous, J. (2022) 'An Interplay between Epigenetics and Translation in Oocyte Maturation and Embryo Development: Assisted Reproduction Perspective', Biomedicines, 10(7). doi: 10.3390/BIOMEDICINES10071689. (REVIEW)

- *Review article with major contribution. It was written with aim to appreciate new findings related to epitranscriptomics and complexity of PCOS in light of lifestyle and environmental factors.*

Zhu, L., Zhou, T., Iyyappan, R., Ming, H., **Dvoran, M.**, Wang, Y., Chen, Q., Roberts, R.M., Susor A., Jiang Z. (2022) 'High-resolution ribosome profiling reveals translational selectivity for transcripts in bovine preimplantation embryo development', Development (Cambridge, England), 149(21). doi: 10.1242/DEV.200819.

Research article with contribution in experimental part, where I mainly took part in polysome fractionation and qPCR data analysis.

del Llano, E., Iyyappan, R., Aleshkina, D., Masek, T., **Dvoran, M.**, Jiang Z., Pospisek, M., Kubelka, M., Susor, A. (2022) 'SGK1 is essential for meiotic resumption in mammalian oocytes', European journal of cell biology, 101(2). doi: 10.1016/J.EJCB.2022.151210.

- *Research article with contribution in experimental part, where I took part in polysome fractionation and proofreading of the revised article.*

Tetkova, A., Susor, A., Kubelka, M., Nemcova, L., Jansova, D., **Dvoran, M.**, del Llano, E., Holubcova, Z., Kalous, J. (2019) 'Follicle-stimulating hormone administration affects amino acid metabolism in mammalian oocytes†', Biology of reproduction, 101(4), pp. 719–732. doi: 10.1093/BIOLRE/IOZ117.

- *Research article with contribution in experimental part, where I created supplementary data for spindle measurements of rFSH treated MII oocytes from naturally or PMSG stimulated female mice. I also performed thawing of vitrified human GV oocytes destined for ^{35}S-methionine labelling.*

9. Abbreviations

AR – assisted reproduction

ART – assisted reproduction technology

AREG – amphiregulin

AURKA – aurora kinase A

BSA – bovine serum albumin

cAMP – cyclic adenosine monophosphate

CCNB1 – cyclin B1

CENPV – centromere protein V

CDK1 – cyclin dependent kinase 1

cGMP – cyclic guanosine monophosphate

DE – differentially expressed

DGE – differential gene expression

EDTA - ethylenediaminetetraacetic acid

EGF - epidermal growth factor

ERK1 - extracellular-signal regulated kinase 1

EVs – extracellular vesicles

FBS – foetal bovine serum

FR – fertilization rate

GnRH – gonadotropin releasing hormone

GO – gene ontology

GOEA – gene ontology enrichment analysis

GV – germinal vesicle oocyte

hCG – human chorionic gonadotropin

IBMX – isobutyl-methyl-xanthine

ICSI – intracytoplasmic sperm injection

IVM DO – *in vitro* matured denuded oocytes

IVM COC – *in vitro* matured cumulus-oocyte complexes

IVO – *in vivo* matured MII oocyte

IMZ – *in vitro* fertilized IVM DO pronuclear zygotes

IVZ – *in vivo* pronuclear zygotes

LBR – live birth rate

MARDO - mitochondria-associated ribonucleoprotein domain

MPF - maturation-promoting factor

mTOR - mechanistic target of rapamycin

mTORC1 - mechanistic target of rapamycin complex 1

NEBD – nuclear envelope breakdown

NSN – non-surrounded nucleolus GV oocyte

NSUN2 – NOP2/Sun RNA methyltransferase 2

OHSS – ovarian hyperstimulation syndrome

OPU – oocyte pick-up

PARN – poly (A) specific ribonuclease

PB – p-body

PBE – polar body extrusion

PCOS – polycystic ovarian syndrome

PKA – protein kinase A

PKB – protein kinase B

PMSG – pregnant mare serum gonadotropin

RNP - ribonucleoprotein

RPKM – reads per kilobase million

SG – stress granule

SPAG5 – sperm associated antigen 5

SN – surrounded nucleolus GV oocyte

SSP – scarce sample profiling

TOP – terminal oligopyrimidine

TZP – transzonal projections

UTR – untranslated region